Accelerator Physics Issues at LHC & Beyond

Frank Zimmermann, CERN, SL/AP

Outline of the Two Lectures

(A) Past and Future

(B) The Large Hadron Collider (LHC)

(C) LHC Upgrades, VLHC-I and II

(A) Past and Future

past, operating, or under construction:

ISR	1970
SPS	1981
Tevatron	1987
RHIC	2000
LHC	2006

contemplated: LHC-II, VLHC HF or LF, and Eloisatron

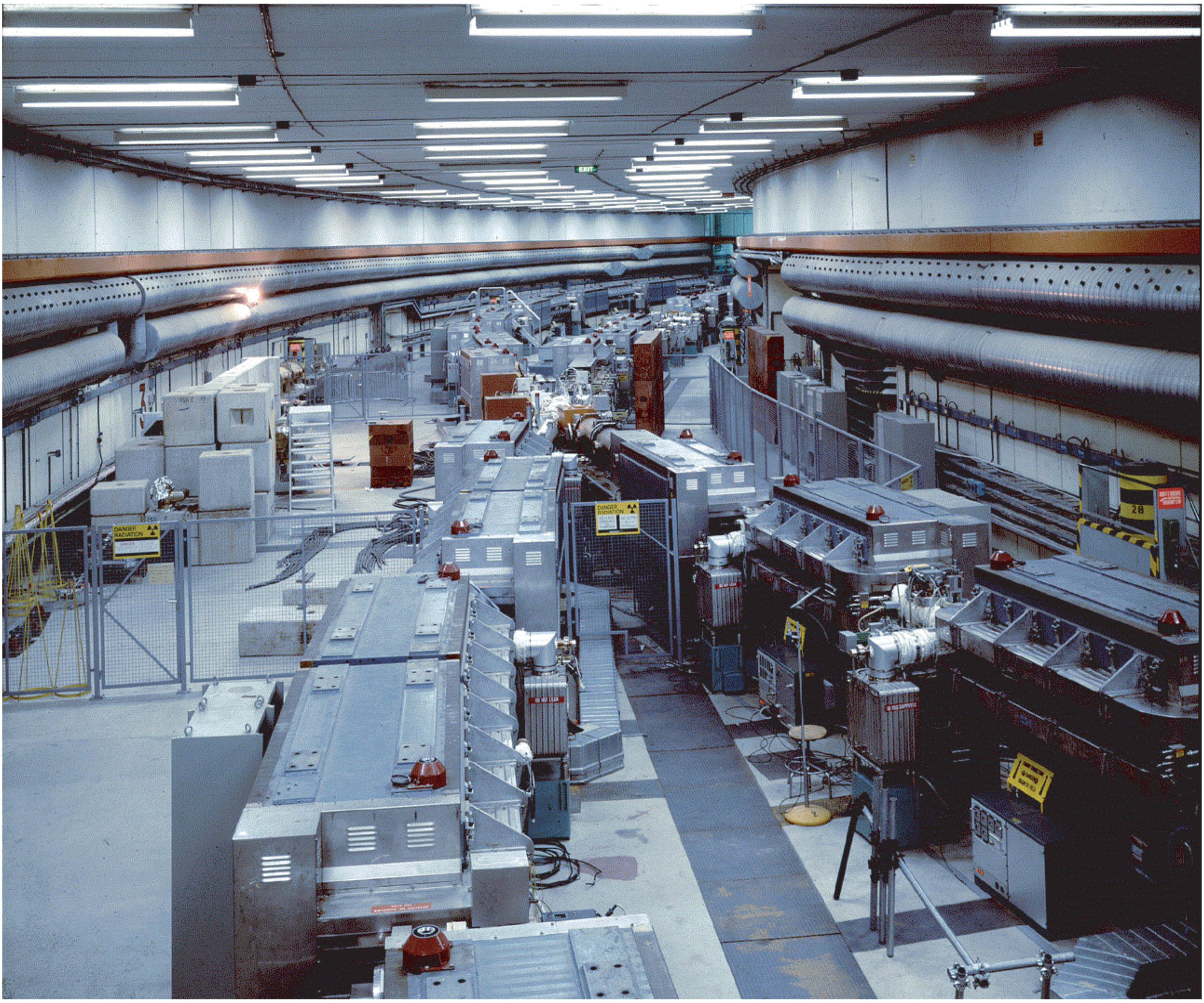
DANGER
RADIATION
DANGER
RADIATION
28

ISR - the first hadron collider!
Limitations and Successes

- space-charge tune shift & spread , **trapped e^-**
- **proton-electron instabilities, pressure bumps**
- detector **background**
- coherent beam-beam effects
- detector missed the J/ψ and b quark
- I =**38–50 A, coasting beam**, 31 GeV
- $L \approx 2.2 \times 10^{32}$ $\mathbf{cm^{-2}s^{-1}}$ peak luminosity
- with bunched beams $\xi = 0.0035$ per IP (8 crossings)
- first $p\bar{p}$ collisions

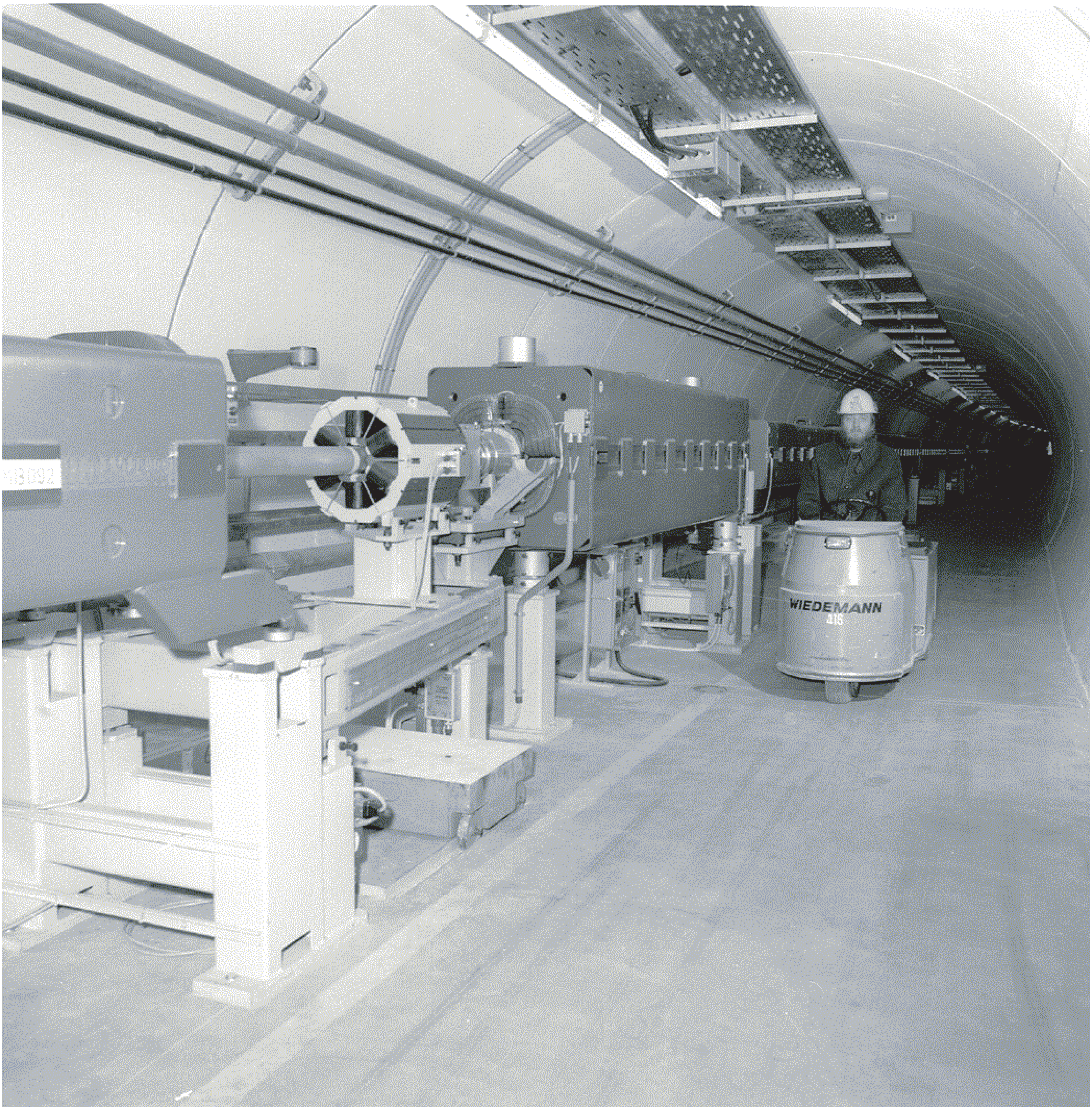
WIEDEMANN
416

Parameters for pp or $p\bar{p}$ Colliders

acc.	$Sp\bar{p}S$	TeV2a	LHC	LHC-II	VLHC-I	VLHC-II
E_{beam} [TeV]	0.32	0.98	7	14	20	87.5
B [T]	1.4	4.34	8.4	16.8	2	9.8
C [km]	6.9	6.28	26.7	26.7	233	233
n_b	6	36	2800	5600	40000	40000
N_b [10^{11}]	1.7 (p)	2.7 (p)	1.05	1.05	0.26	0.075
	0.8 ($\bar{p}$)	~1.0 ($\bar{p}$)				
L [10^{34}cm^{-2}s^{-1}]	0.0006	$\sim$ 0.02	1.00	10.	1.0	2.0
$\beta^*_{x,y}$ [m]	0.6, 0.15	0.35	0.5	0.22	0.3	0.71
$\gamma\epsilon_{x,y}$ [μm]	3.75	$\sim$ 3	3.75	3.75	1.5	1.6
				→1.0		→0.04

Empirical Scaling

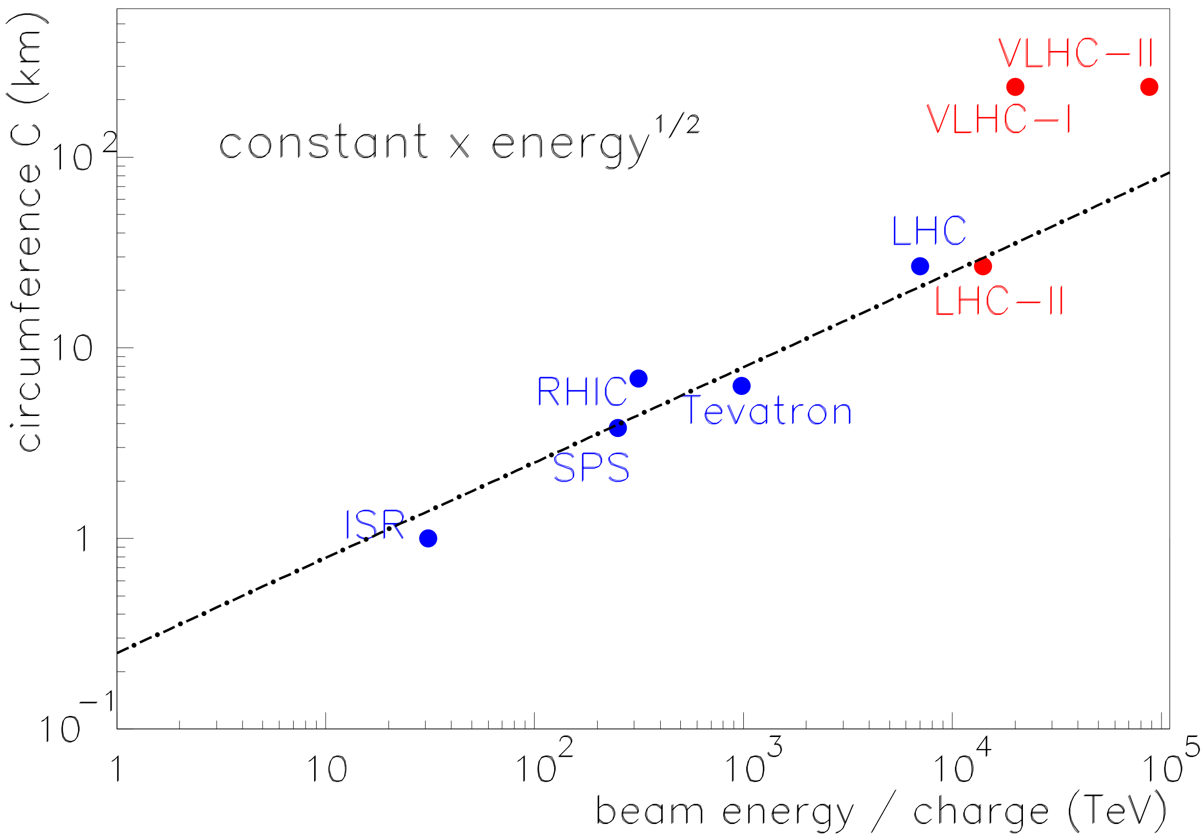

Circumference vs. beam energy: $C \propto E^{1/2}$

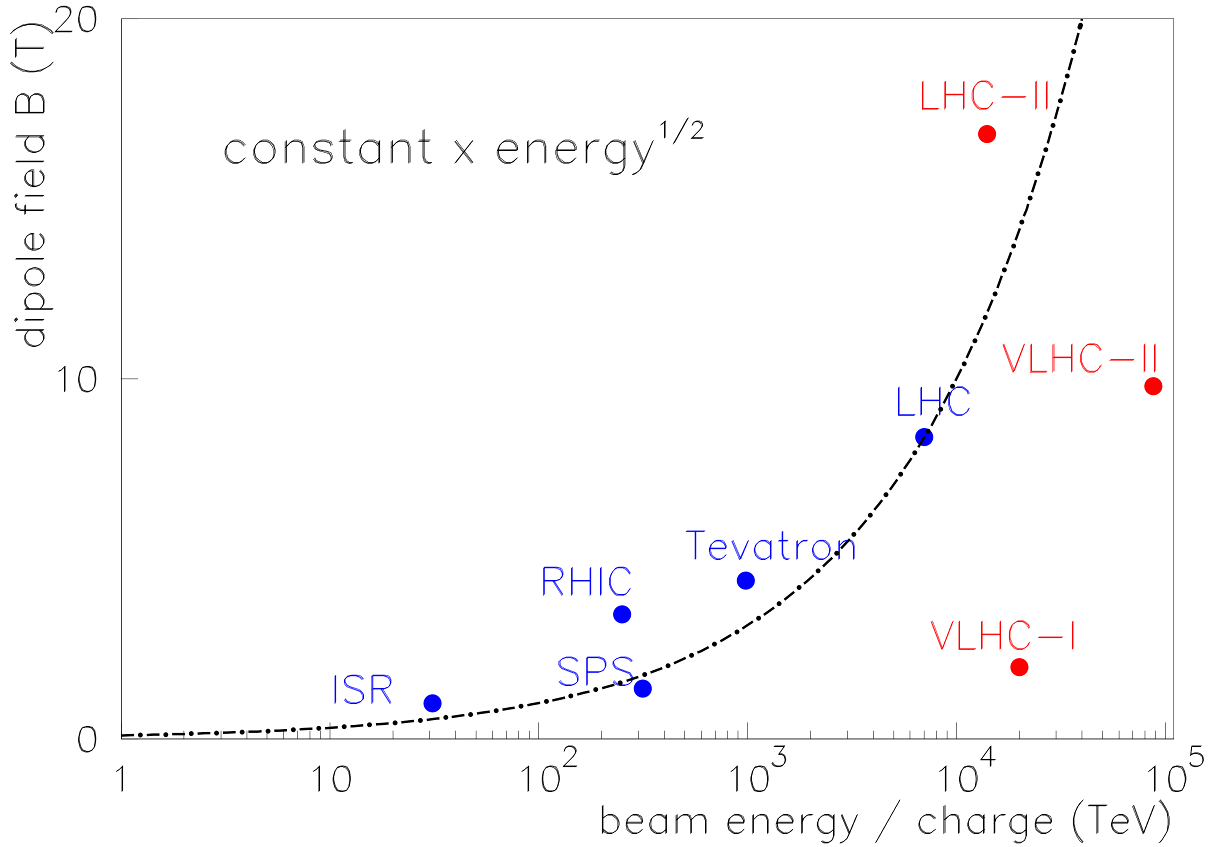

Dipole field vs. beam energy: $B \propto E^{1/2}$

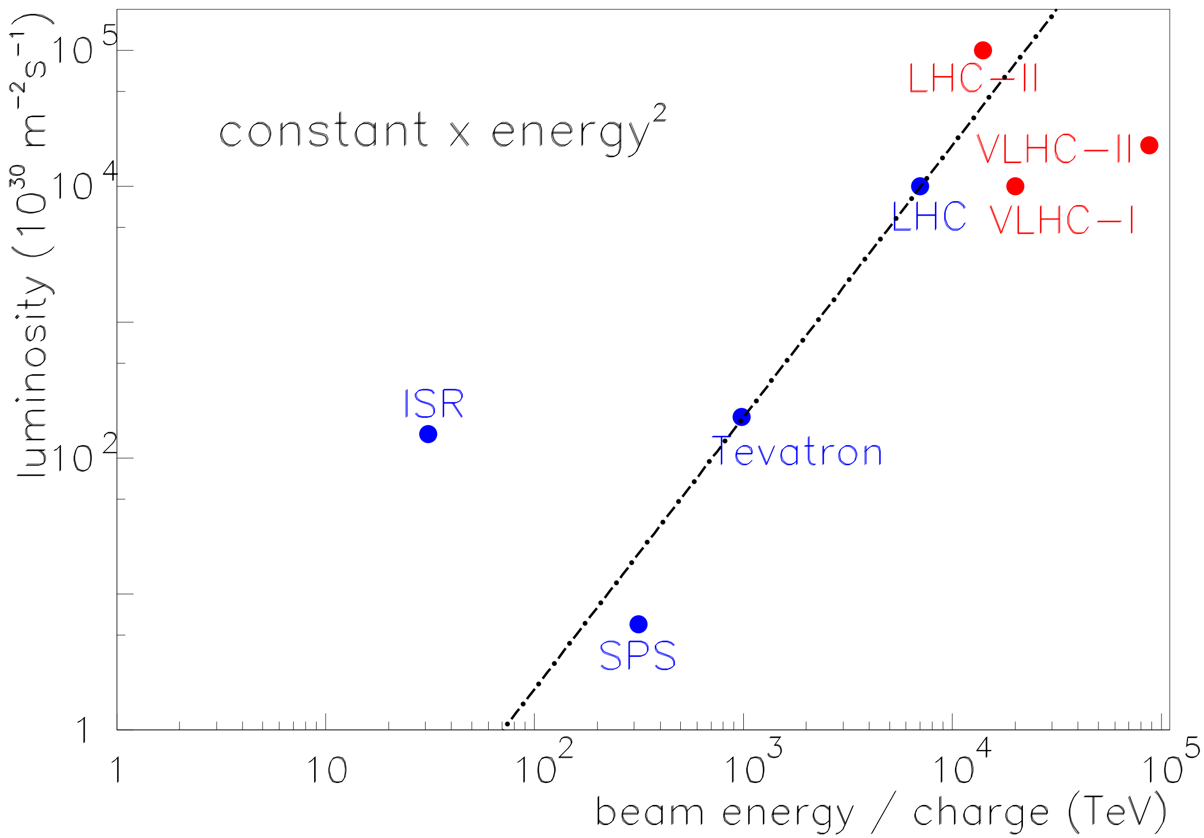

Luminosity vs. beam energy: $L \propto E^2$ event rate = luminosity $\times$ cross section

accelerator physics fundamentals

stored particles execute transverse betatron oscillations

$$\frac{d^2x}{ds^2} = -k(s)\ x$$

with quadrupole focusing force k [m^{-2}]:

$$k = \frac{eB_T}{pa}$$

(B_T: pole-tip field, a: radius, p: momentum)

Betatron Tune: number of betatron oscillations per turn

Emittance: phase space area of beam distribution $\epsilon = \int x'\ dx\ /\pi$ ($x' \equiv dx/ds$); $\gamma\epsilon$ is invariant under acceleration ('normalized emittance')

Beta function: determines local rms beam size:

$$\sigma_{x,y}(s) = \sqrt{\beta_{x,y}(s)\epsilon_{x,y}}$$

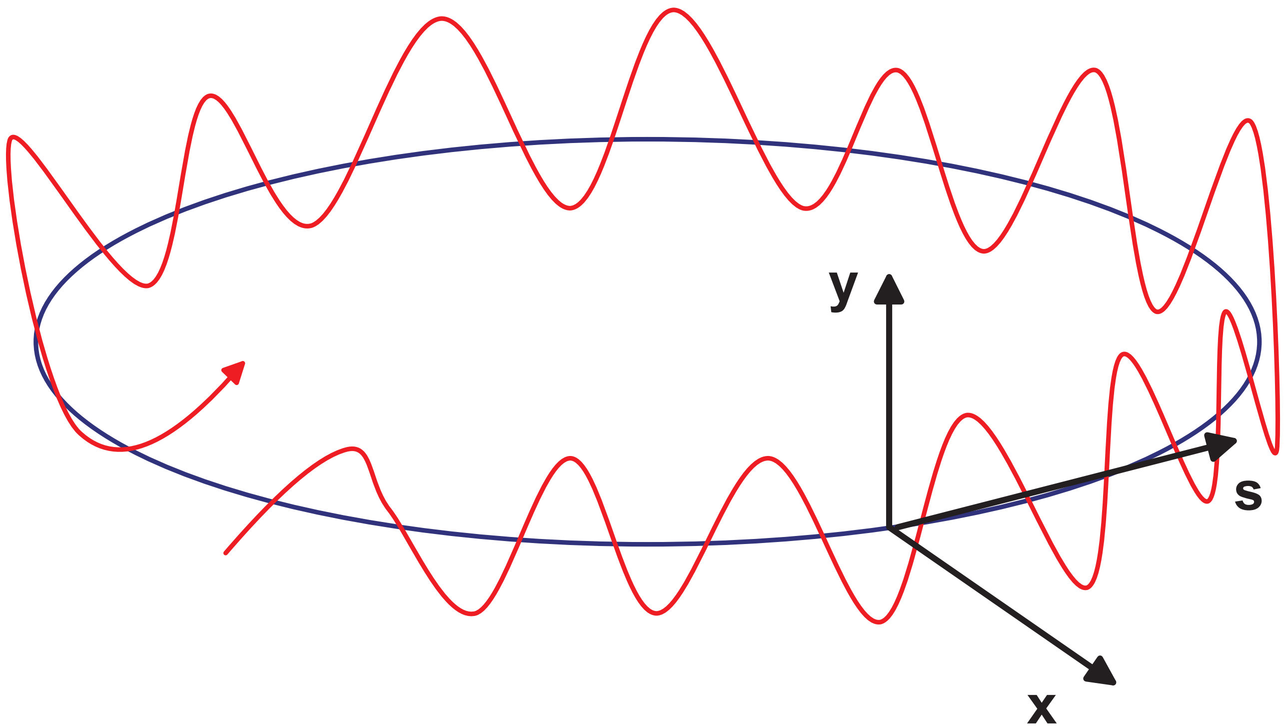

Betatron tune $Q_{x,y}$ equals the number of transverse oscillations per revolution. Avoid resonances $kQ_x + mQ_y = p$ $(k, m, p$ integers)! [CERN SPS: $|k| + |m| \leq 12 \rightarrow$ poor lifetime]

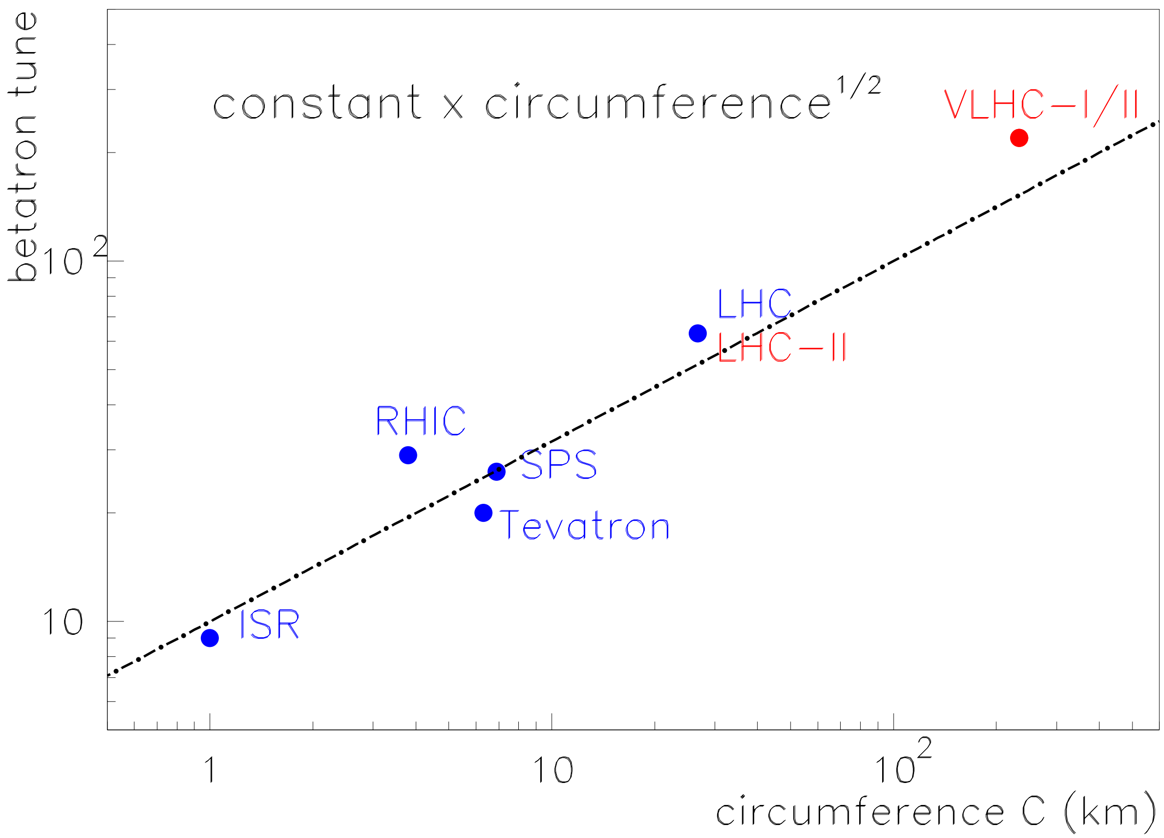

Betatron tune vs. circumference: $Q_\beta \propto C^{1/2}$

$(\rightarrow L_{\rm cell} \propto C^{1/2},\ \beta \propto C^{1/2})$.

(B) The Large Hadron Collider (LHC)

- parameter choice
- magnets, schedule, layout & optics
- head-on beam-beam interaction & luminosity
- long-range collisions
- strong-strong beam-beam & Landau damping
- dynamic aperture, snap-back, power converters, novel diagnostics
- heat load, collimation, vacuum system
- protection & beam dump
- filling pattern, (pre-)injectors, ion collisions
- electron cloud

LHC Parameter Choice

- LEP circumference + highest magnetic field $E[\text{TeV}] \approx 0.84\ B[\text{T}] \rightarrow$ beam energy = 7 TeV with $B = 8.4$ T
- maximum 'beam-beam tune shift' $\xi \propto N/\epsilon$ + available aperture $\rightarrow$ bunch population
- desired luminosity $\rightarrow$ number of bunches $\rightarrow$ beam current, synchrotron radiation power

LHC S.C. Dipole Magnets

accelerator	dipole field
SPS	1.8 T
Tevatron	4 T
HERA	5 T
SSC	6 T
LHC	8.4 T

Persistent Currents

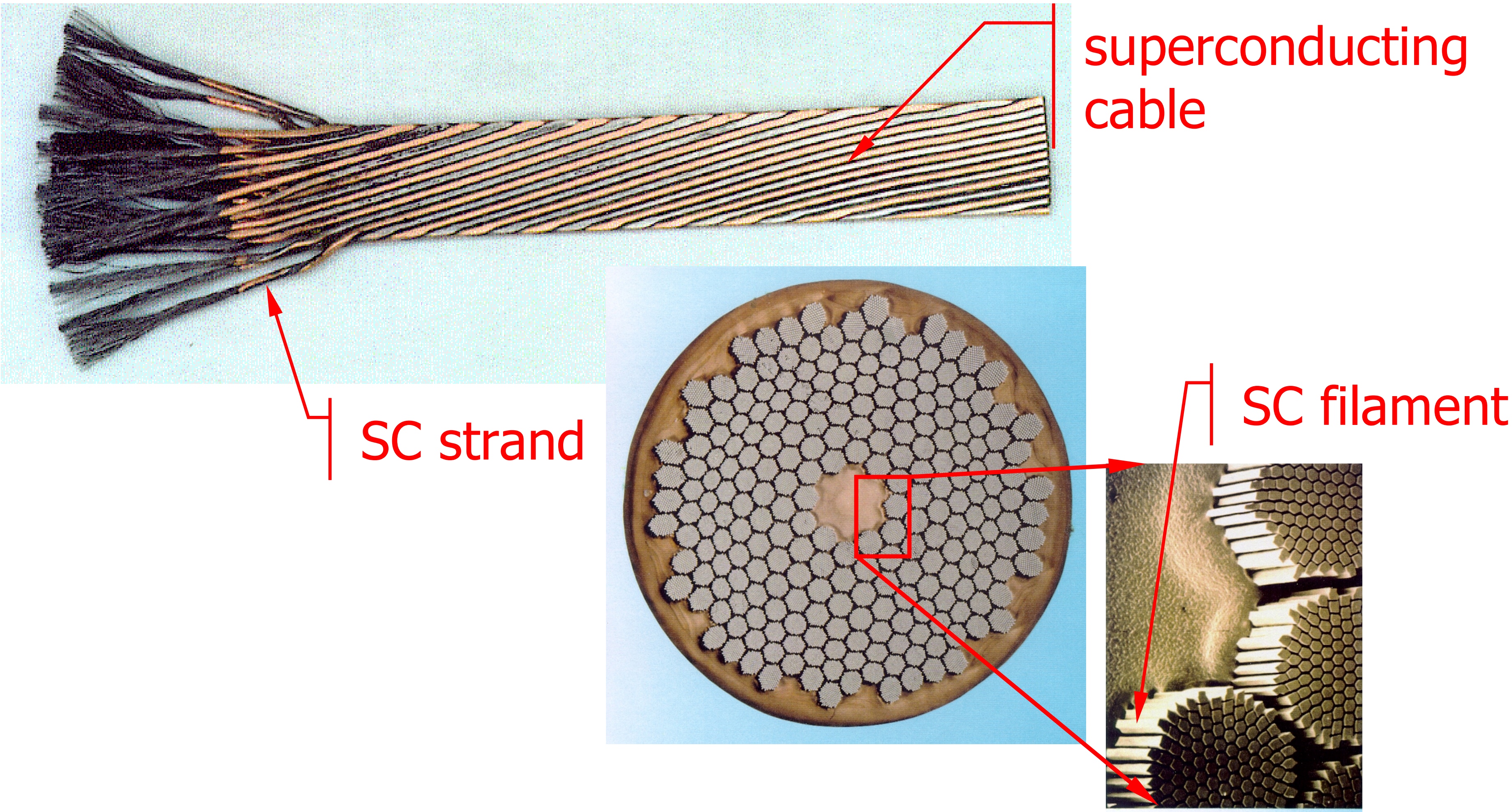

dipole magnet basics

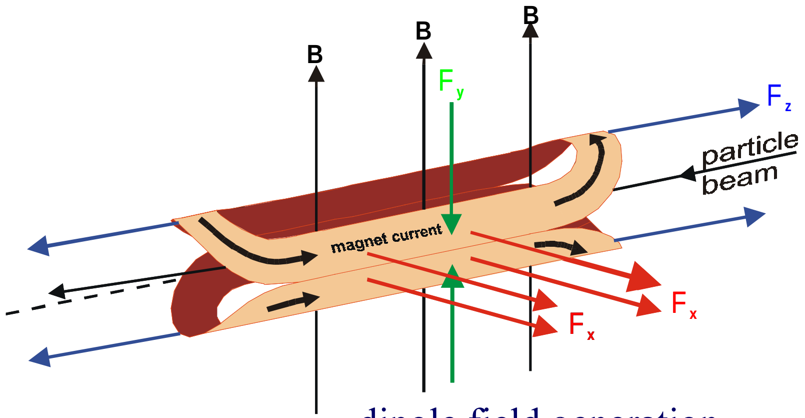

dipole field generation

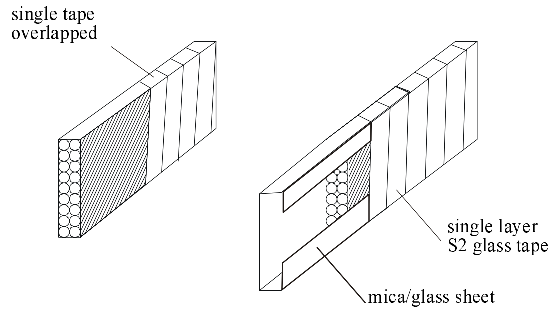

cable and insulation

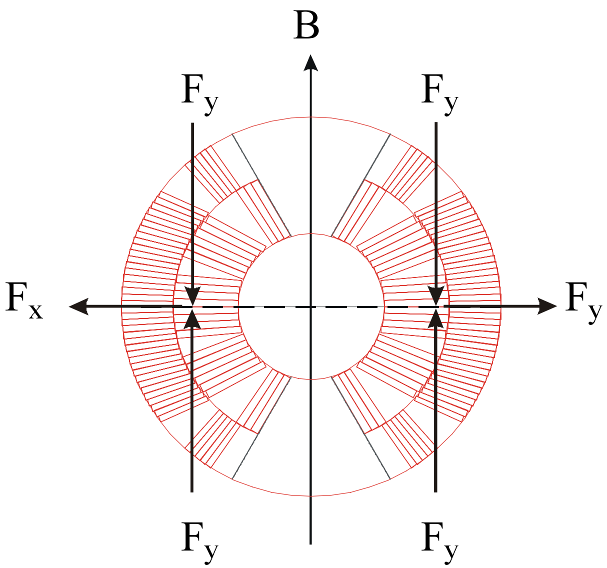

conductor lay-out

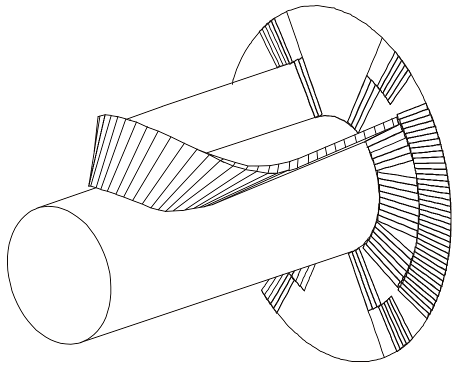

coil winding

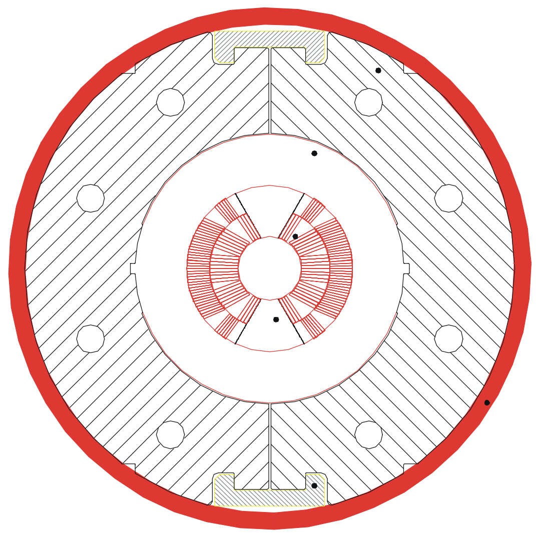

support structure

LHC DIPOLE : STANDARD CROSS-SECTION

CERN AC/DI/MM - HE107 - 30 04 1999

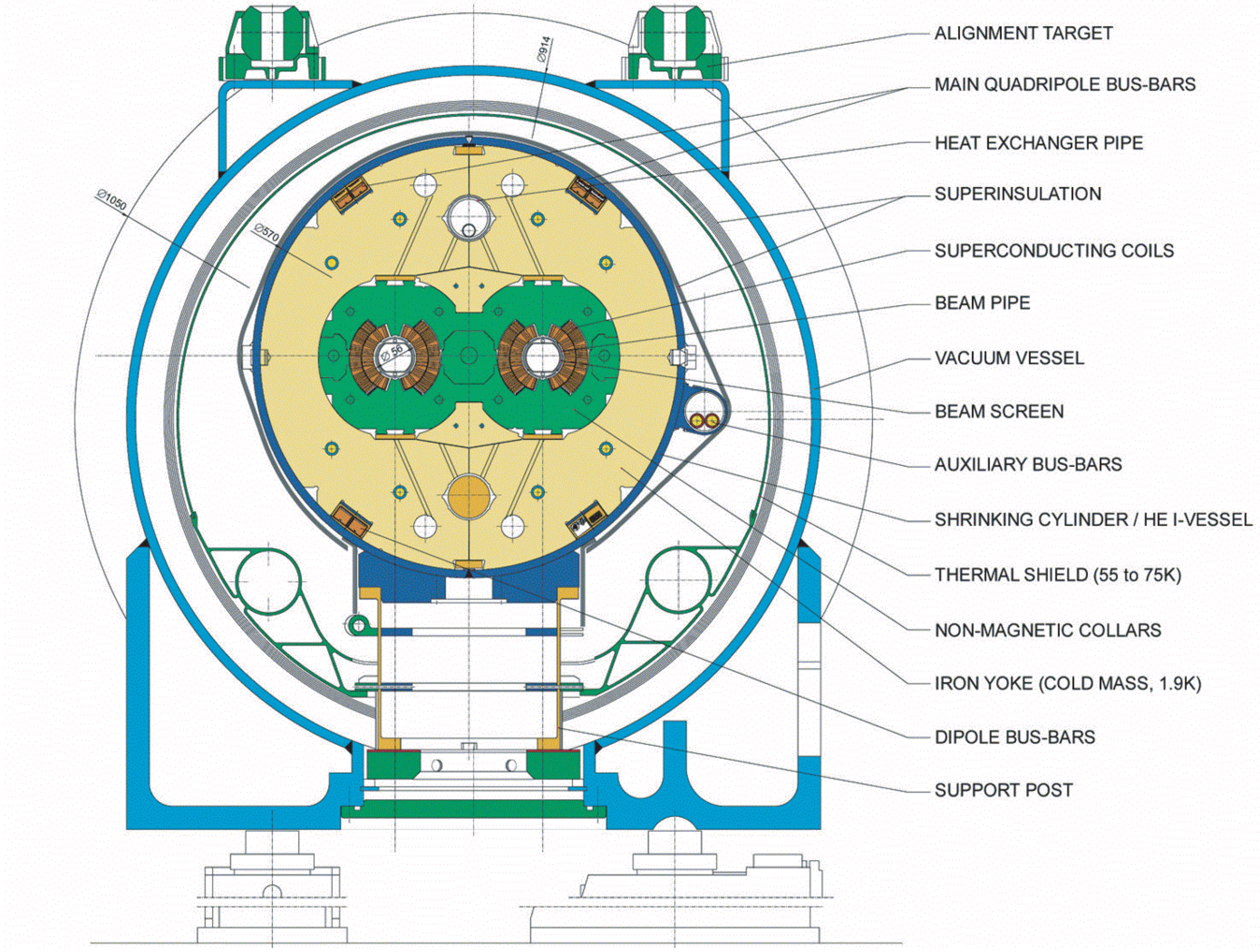

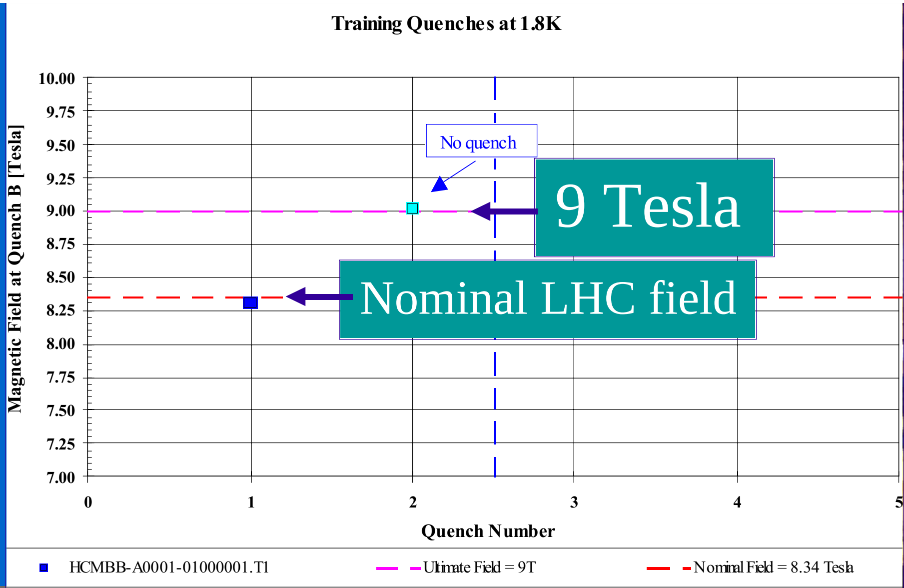

The LHC dipole n. 0001

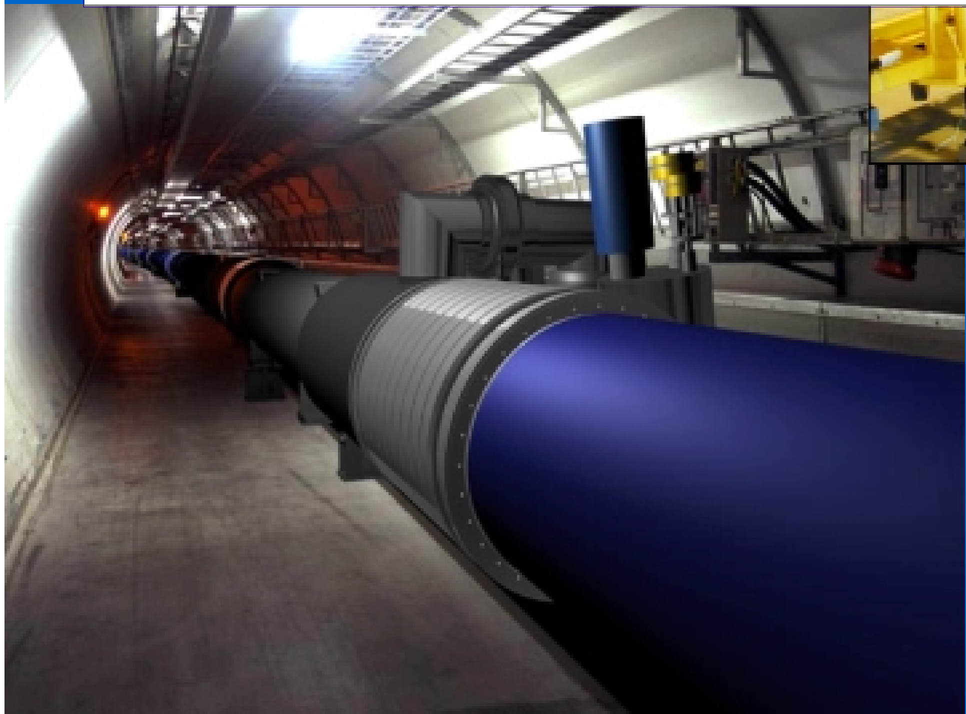

Artist view of the LHC in the LE P Tunnel

LHC commissioning schedule

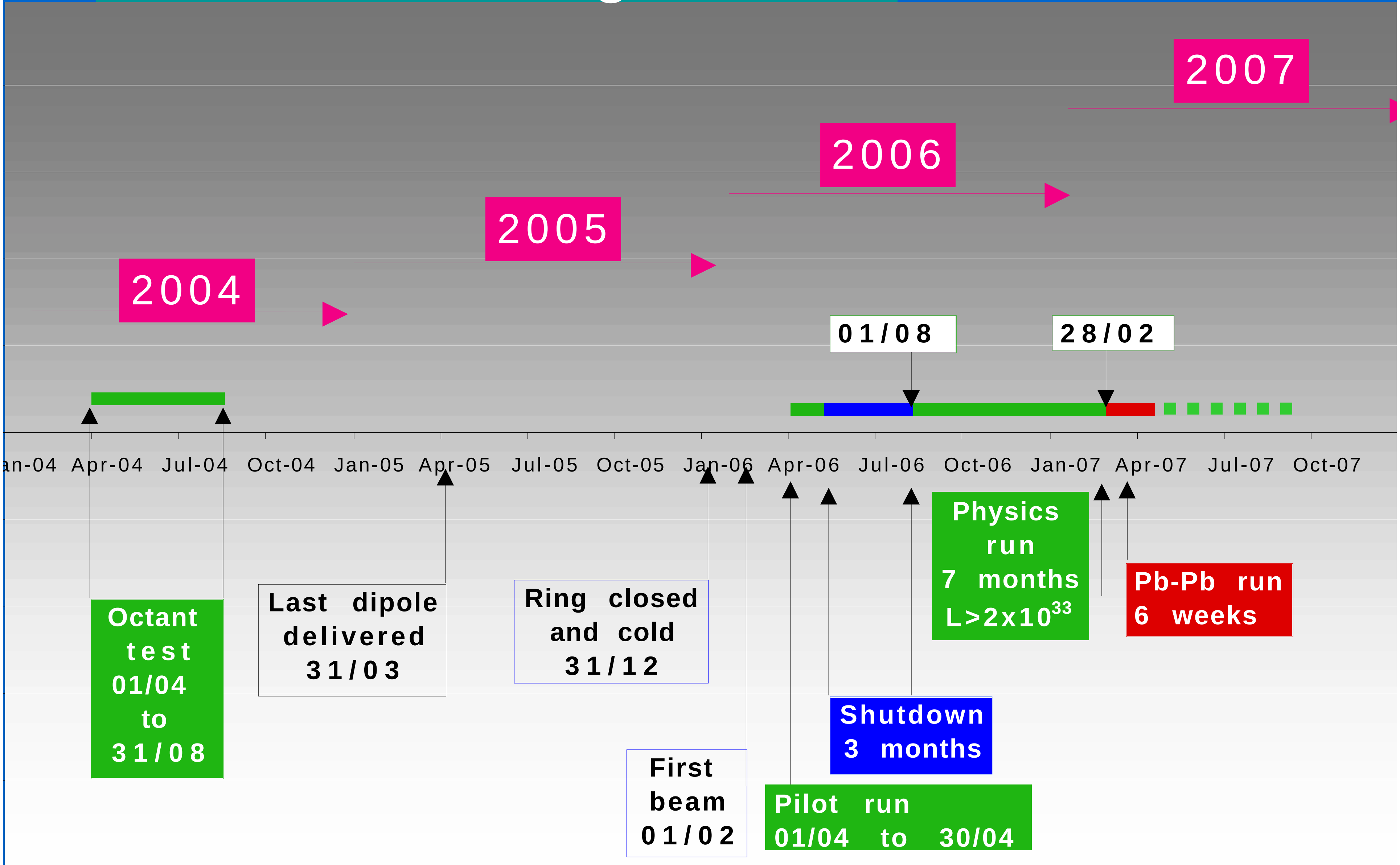

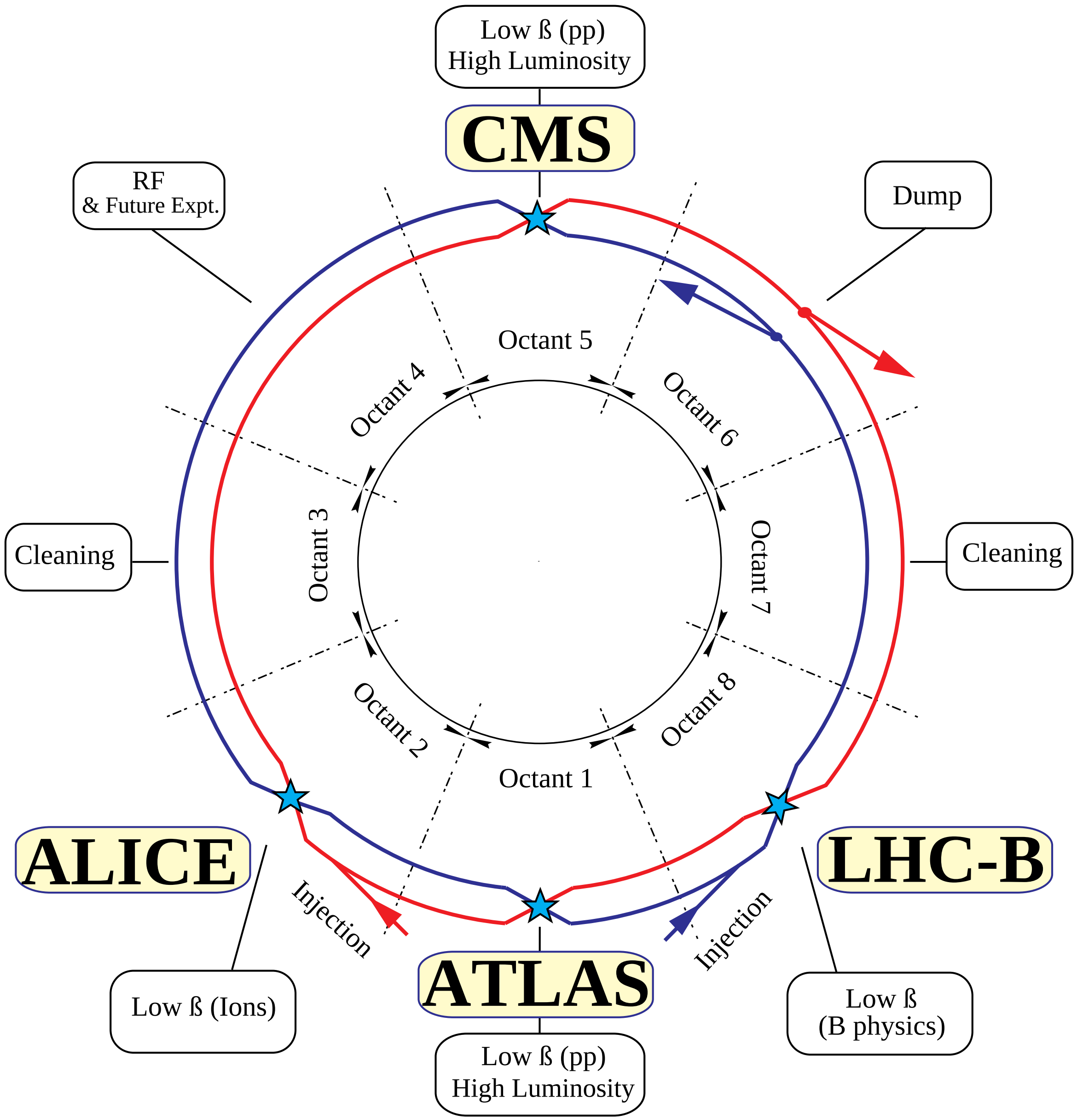
Low ß (pp)
High Luminosity
CMS
RF
& Future Expt.
Dump
Octant 5
Octant 4
Octant 6
Cleaning
Octant 3
Octant 7
Cleaning
Octant 2
Octant 8
Octant 1
ALICE
LHC-B
Injection
Injection
ATLAS
Low ß (Ions)
Low ß
(B physics)
Low ß (pp)
High Luminosity

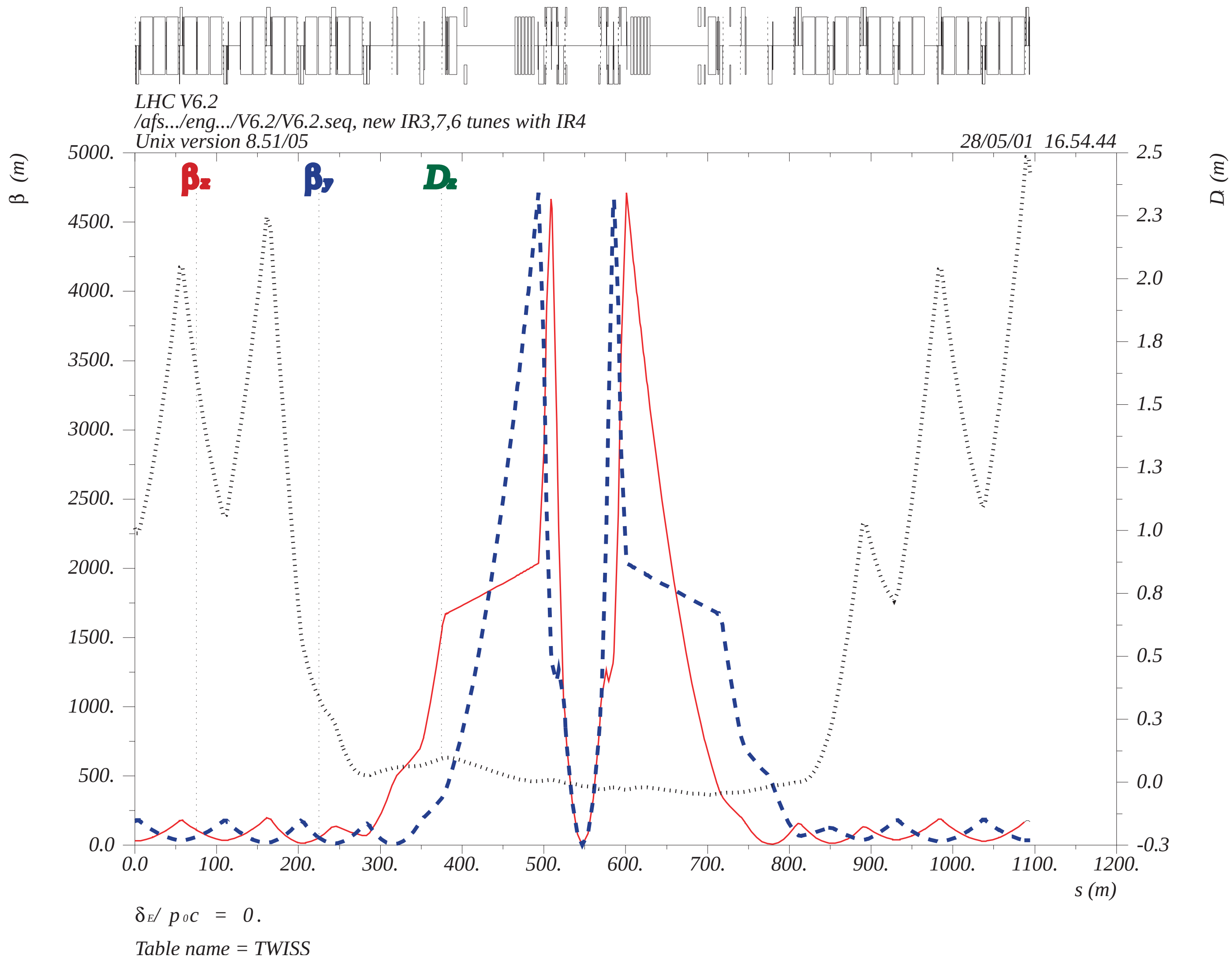

Collision lattice for beam 1 at IP5 ($x = D\Delta p/p + x_\beta$).

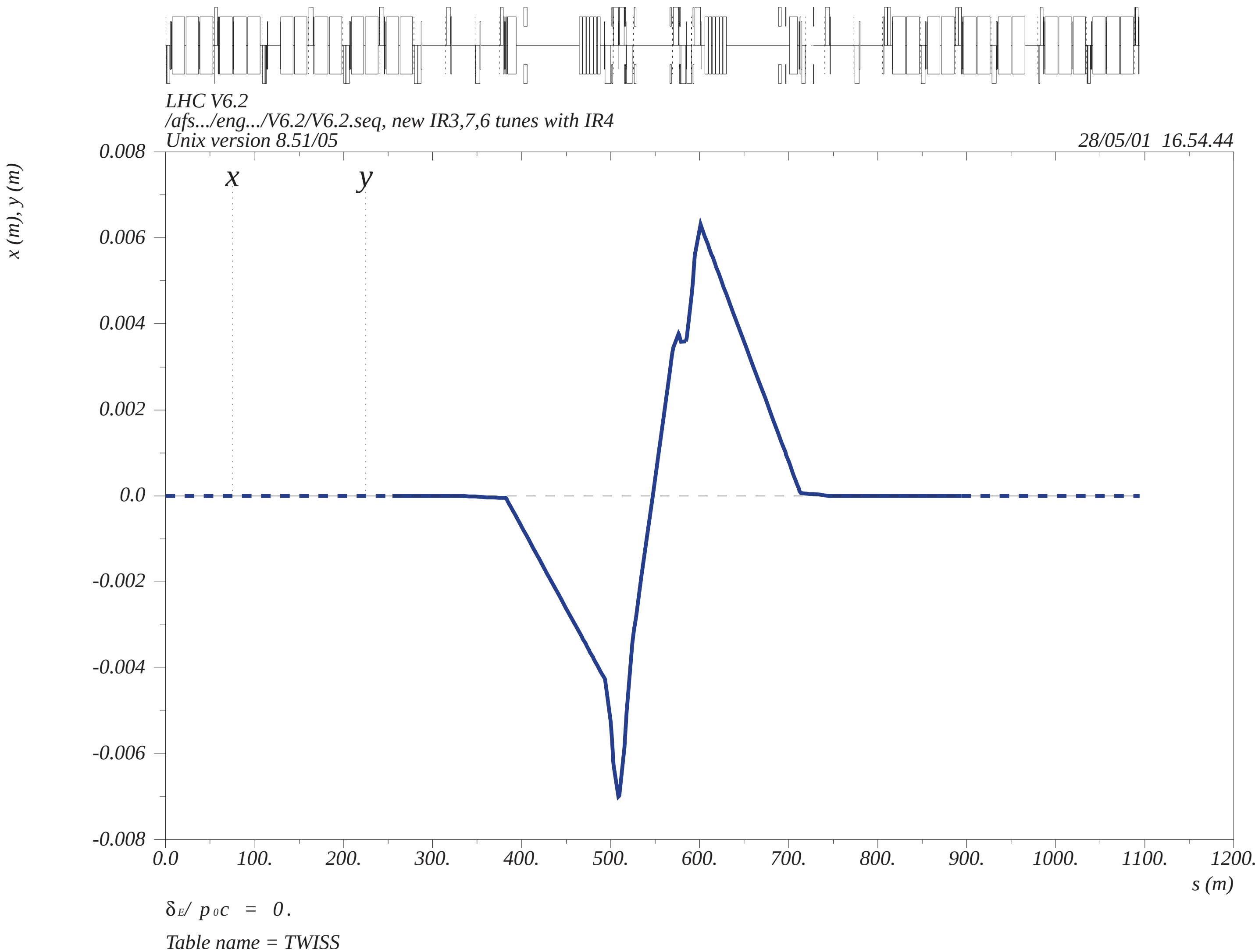

LHC design orbit for beam 1 near IP5 (CMS) in collision.

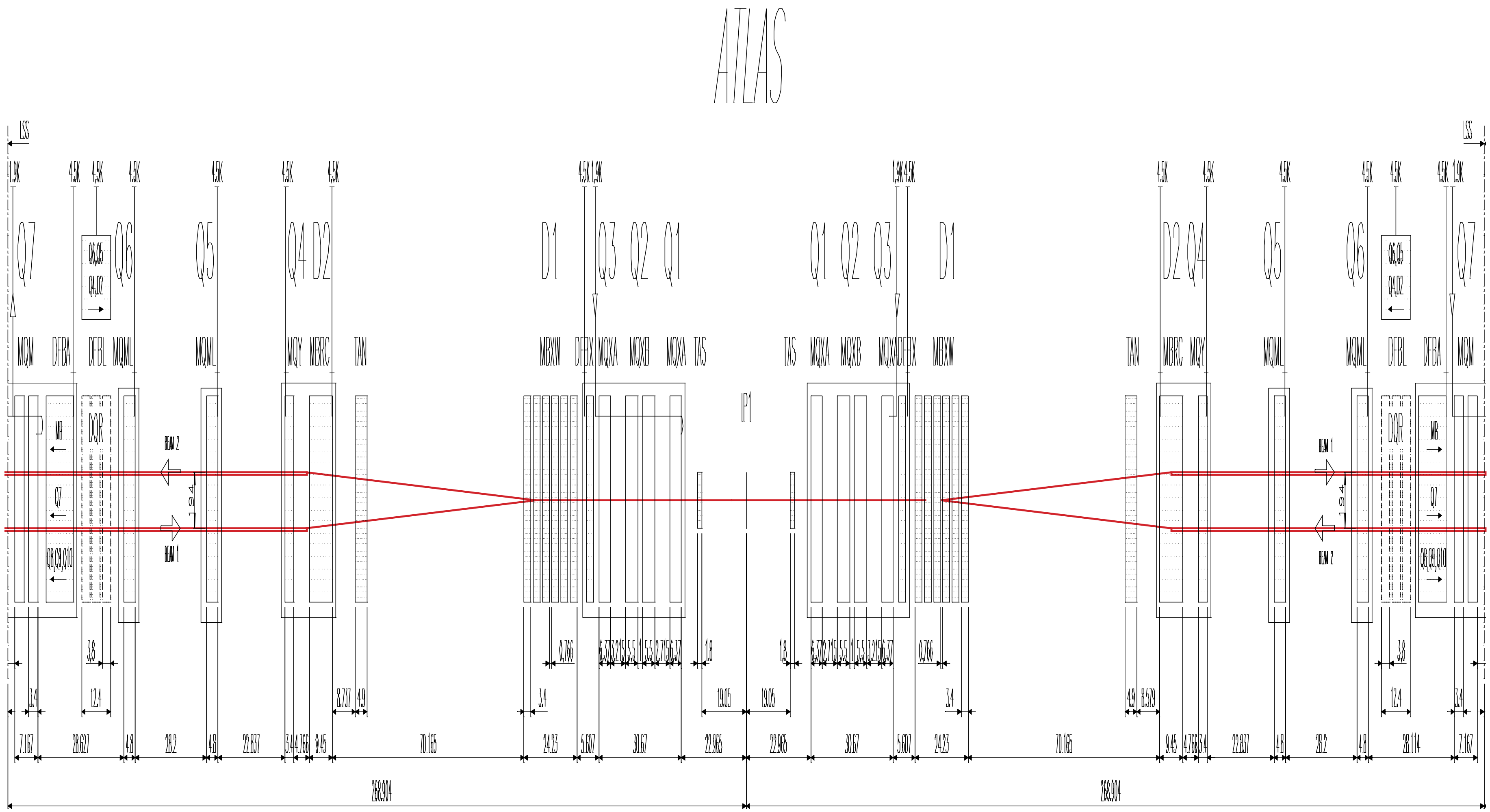

Magnet layout (top view) around IP 1 (ATLAS).

Head-On Beam-Beam Collision

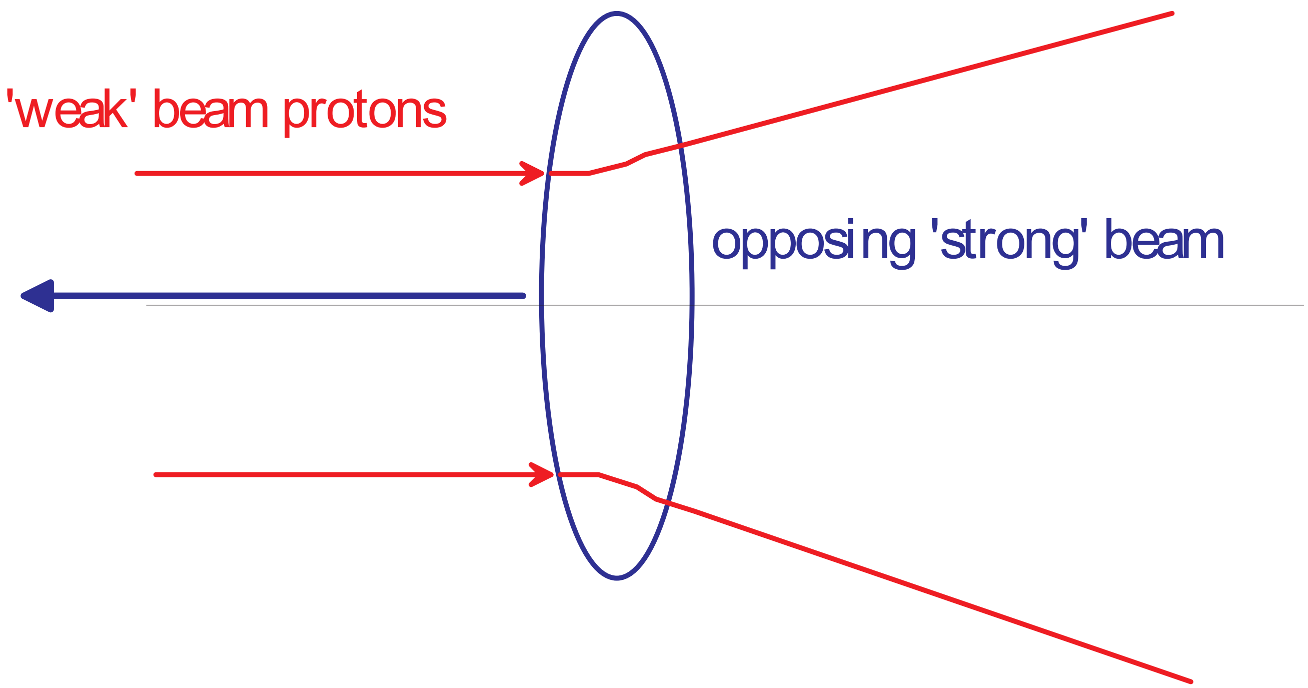

Repelling force of opposing beam acts like defocusing lens $\rightarrow Q_{x,y}$ decreases

nonlinear lens $\rightarrow$ tune spread

maximum acceptable tune spread $\rightarrow$ beam-beam limit.

$\Delta Q_{x,y}$ is characterized by the beam-beam tune shift parameter:

$$\Delta Q_{x,y} \approx \xi_{x,y} \equiv \frac{r_p \beta^*_{x,y} N_b}{2\pi\gamma\sigma^*_{x,y}(\sigma^*_x + \sigma^*_y)}$$

Compare tune shift caused by a quadrupole of strength ΔK:

$$\Delta Q \approx \frac{1}{4\pi}\beta\ \Delta K$$

and take $\Delta K = \Delta x'/x$ (or $\Delta y'/y$) as the kick imparted by the opposing beam.

Comparison of Beam-Beam Tune Shifts

	SPS	TeV-IIa	LHC
ξ/IP	0.005	0.01	0.0034
$\xi_{\rm tot}$	0.015	0.01	0.009

Luminosity

Reaction rate $R = L\sigma$ (σ: cross section)

Standard expression for L:

$$\mathbf{L} = \frac{\mathbf{N_b^2 n_b f_{rev}}\gamma}{\mathbf{4}\pi\sigma^*_{\mathbf{y}}\sigma^*_{\mathbf{x}}} = \frac{\mathbf{N_b^2 n_b f_{rev}}\gamma}{\mathbf{4}\pi\epsilon_{\mathbf{x,N}}\beta^*_{\mathbf{x}}\kappa}$$

N_b: bunch population, n_b number of bunches, $f_{\rm rev}$ revolution frequency, γ beam energy divided by rest mass, $\epsilon_{x,N} = \gamma\epsilon_x$ normalized emittance, and $\kappa = \sigma_y/\sigma_x$ aspect ratio.

head-on beam-beam tune shift:

$$\xi_{\mathbf{x,y}} = \frac{\beta^*_{\mathbf{x,y}}\mathbf{r_p N_b}}{\mathbf{2}\pi\gamma\sigma^*_{\mathbf{x,y}}(\sigma^*_{\mathbf{x}} + \sigma^*_{\mathbf{y}})} = \frac{\mathbf{r_p N_b}}{\mathbf{2}\pi\gamma\epsilon_{\mathbf{x}}(\mathbf{1} + \kappa)}$$

Assuming $\beta_y^*/\beta_x^* = \epsilon_y/\epsilon_x = \kappa \rightarrow \xi_x = \xi_y \equiv \xi$:

$$\mathbf{L} = (\mathbf{f}_{\text{rev}}\mathbf{n_b}\mathbf{N_b})\ \frac{\mathbf{1}+\kappa}{\beta_{\mathbf{y}}^*}\ \gamma\frac{\xi}{\mathbf{2r_p}}$$

Four factors:

- emittance ratio κ
- IP beta function $\beta_y^* = \beta_x^*\kappa$
- maximum beam-beam tune shift ξ
- total beam current $f_{\text{rev}}n_bN_b$

Flat beams: $\kappa \ll 1$ and $L_{\text{flat}} \approx L_{\text{round}}/2$, unless β_y^* can be reduced. (This seems difficult for *pp* colliders.)

Long-Range Collisions

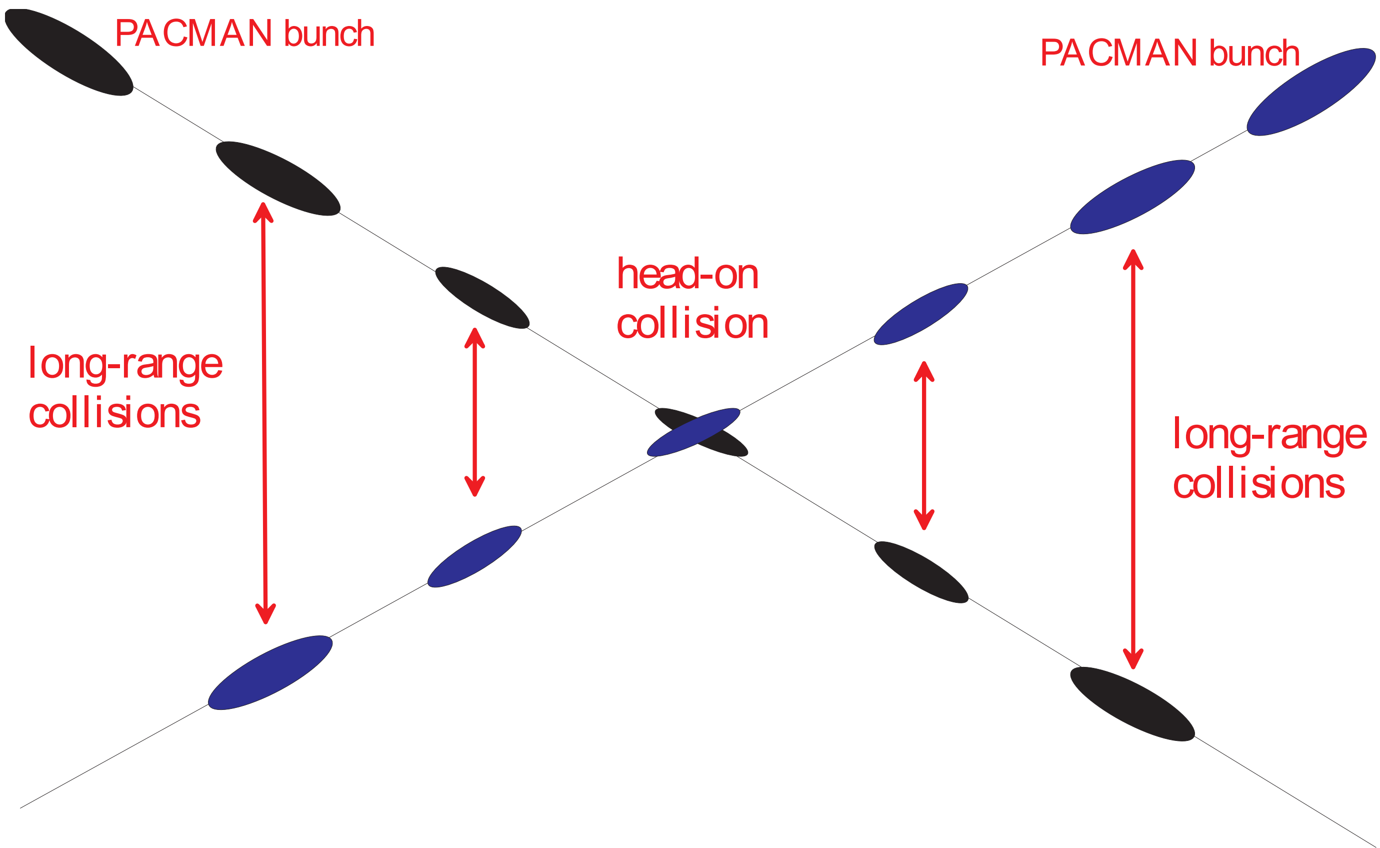

Each bunch experiences up to 15 long-range collisions on either side of each head-on collision. Bunches with an unequal number of encounters will likely have a poor lifetime (PACMAN bunches).

Weak-Strong Beam-Beam Effects at LHC

new regime of beam-beam interaction: long-range encounters on either side of the interaction points are the dominant perturbation, rather than the head-on collisions. The long-range collisions give rise to a well defined diffusive aperture

$$x_{da} = x_{sep} - \Delta \quad \text{with} \quad \frac{\Delta}{\sigma} \propto \sqrt{\frac{N_b}{A\epsilon_N}} Z$$

where x_{sep} denotes the beam-beam separation. The diffusive aperture in units of σ is independent of the beta function and the beam energy. For nominal LHC parameters: $x_{sep} \approx 9.5\sigma$ and $x_{da} \approx 6\sigma$.

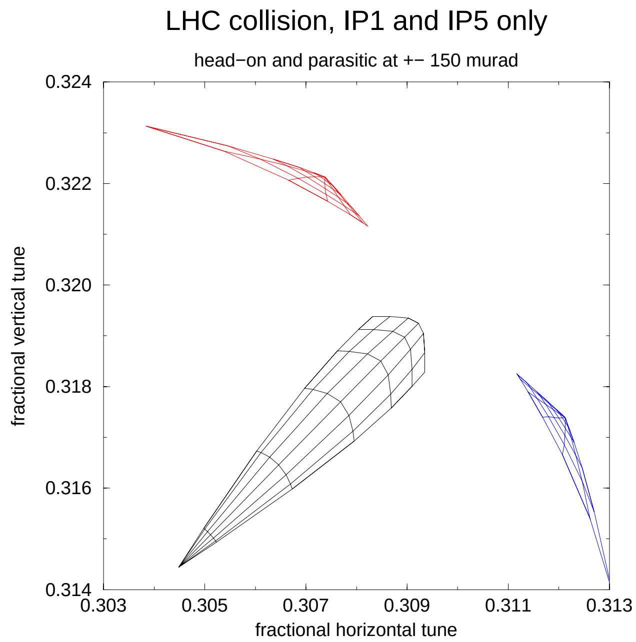

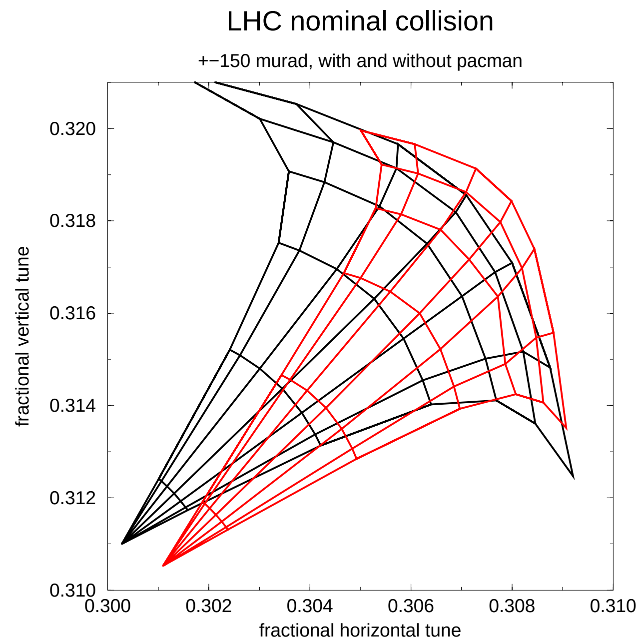

Left: tune footprints due to head-on and long-range beam-beam effects in LHC IPs 1 and 5. Right: total tune footprint in LHC for regular bunch and for PACMAN bunch. [Courtesy H. Grote]. ΔQ from long-range collisions is approx. cancelled by **alternating crossing** at IP 1 and 5.

LHC tune footprints with head-on & long-range collisions and triplet errors (work with Y. Papaphilippou)

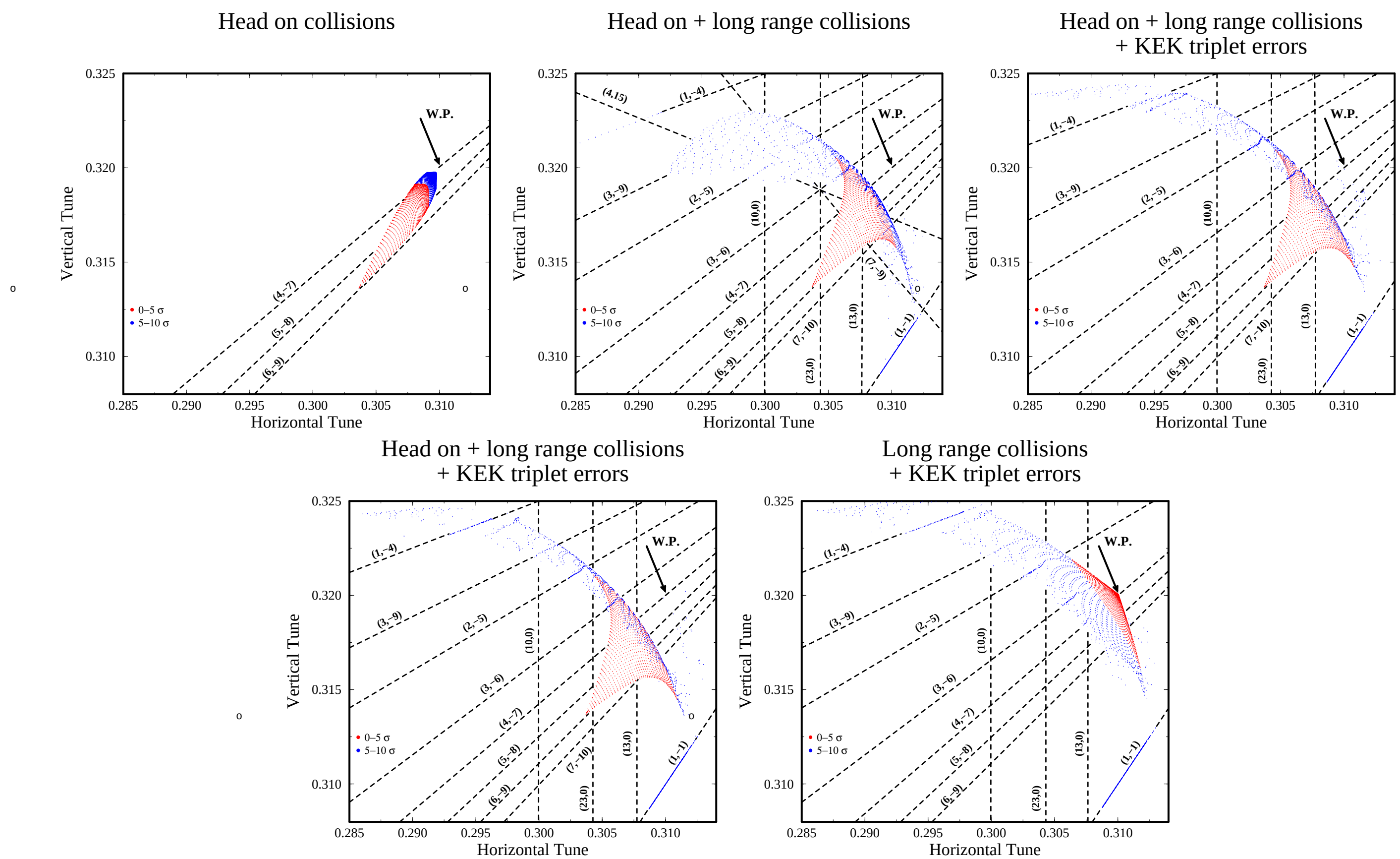

Red dots: x, y_{in} up to $5\sigma_{x,y}$; blue dots: x, y_{in} up to 10 $\sigma_{x,y}$.

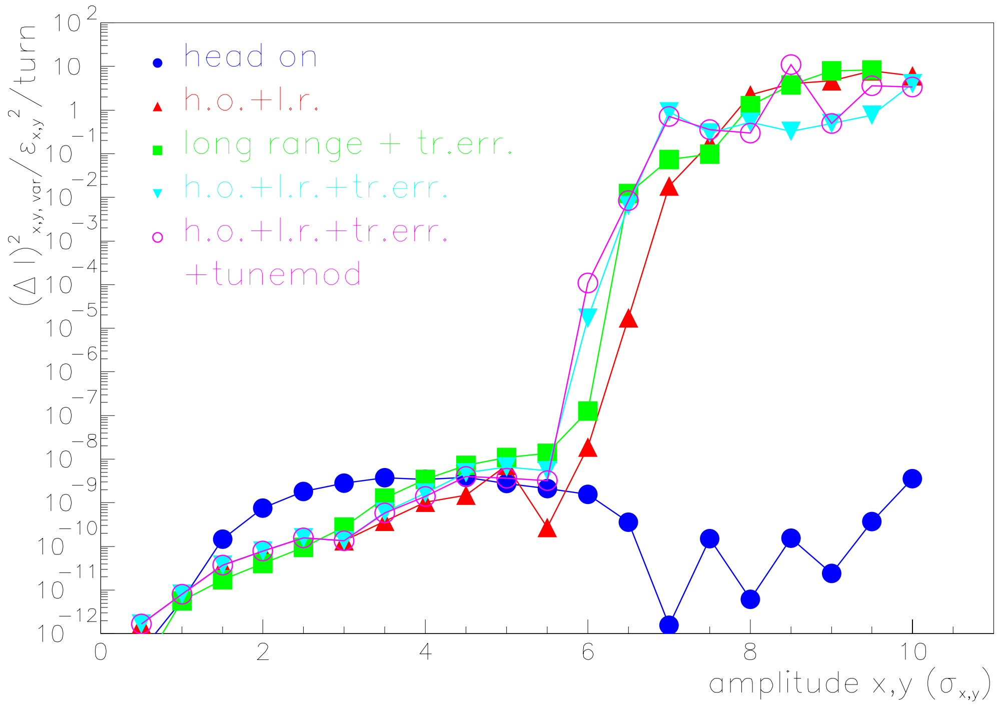

Change of action variance per turn as a function of starting amplitude, for the LHC. Compared are different combinations of head-on collisions, long-range collisions, triplet-field errors, tune modulation, and Moebius twist (Y. Papaphilippou & F.Z.)

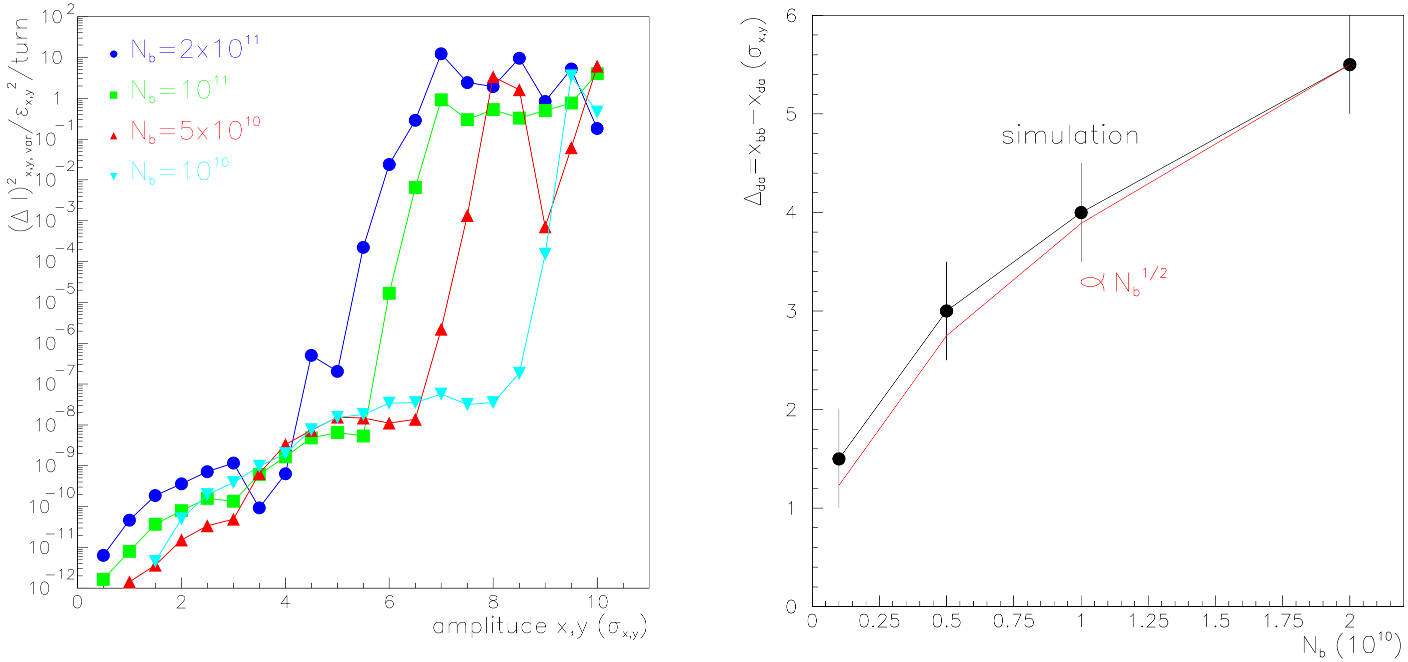

Dependence of diffusion due to long-range collisions on the beam current. Left: change of action variance per turn vs. bunch population; right: approximate diffusive aperture vs. bunch population; vertical axis distance to other beam at parasitic collision point; a square root dependence is also indicated for comparison (Y. Papaphilippou & F.Z.)

Minimum β^*

1st limit — hourglass effect: $\beta^*_{\mathbf{x,y}} \geq \sigma_{\mathbf{z}}$

$(\beta_{x,y}(s) = \beta^*_{x,y} + s^2/\beta^*)$

2nd limit — long-range collisions:

dynamic aperture caused by parasitic collisions

$x_{\rm da} \approx n_{\rm sep}\sigma_x - \Delta \rightarrow n_{\rm sep} \geq 10$; for LHC: $\Delta \approx 3.5\sigma_x$

luminosity loss due to crossing angle:

$$\theta_c \equiv n_{\rm sep}\sqrt{\frac{\epsilon_{x,y}}{\beta^*_{x,y}}} < 2\sigma_x/\sigma_z$$

combining these two equations

$$\beta^*_{\mathbf{x,y}} \geq \mathbf{n}_{\rm sep}\sigma_{\mathbf{z}}/\mathbf{2} \approx \mathbf{5}\sigma_{\mathbf{z}}$$

for the LHC $\beta^*_{x,y} > 0.38$ m (design value 0.5 m)

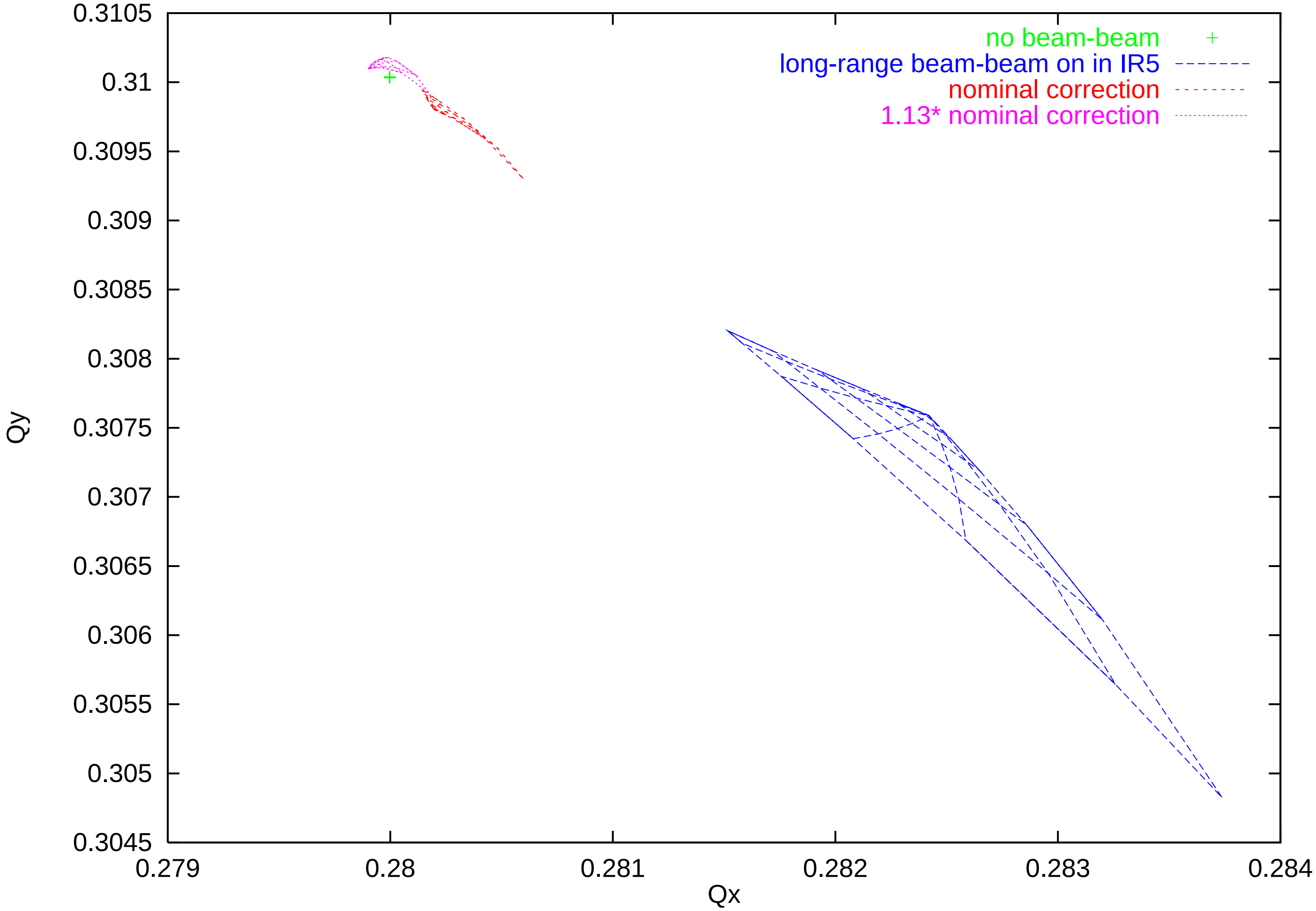

Minimization of tune footprint using pulsed electric wire mimicing long-range encounters of opposite charge [J.-P. Koutchouk, PAC2001]

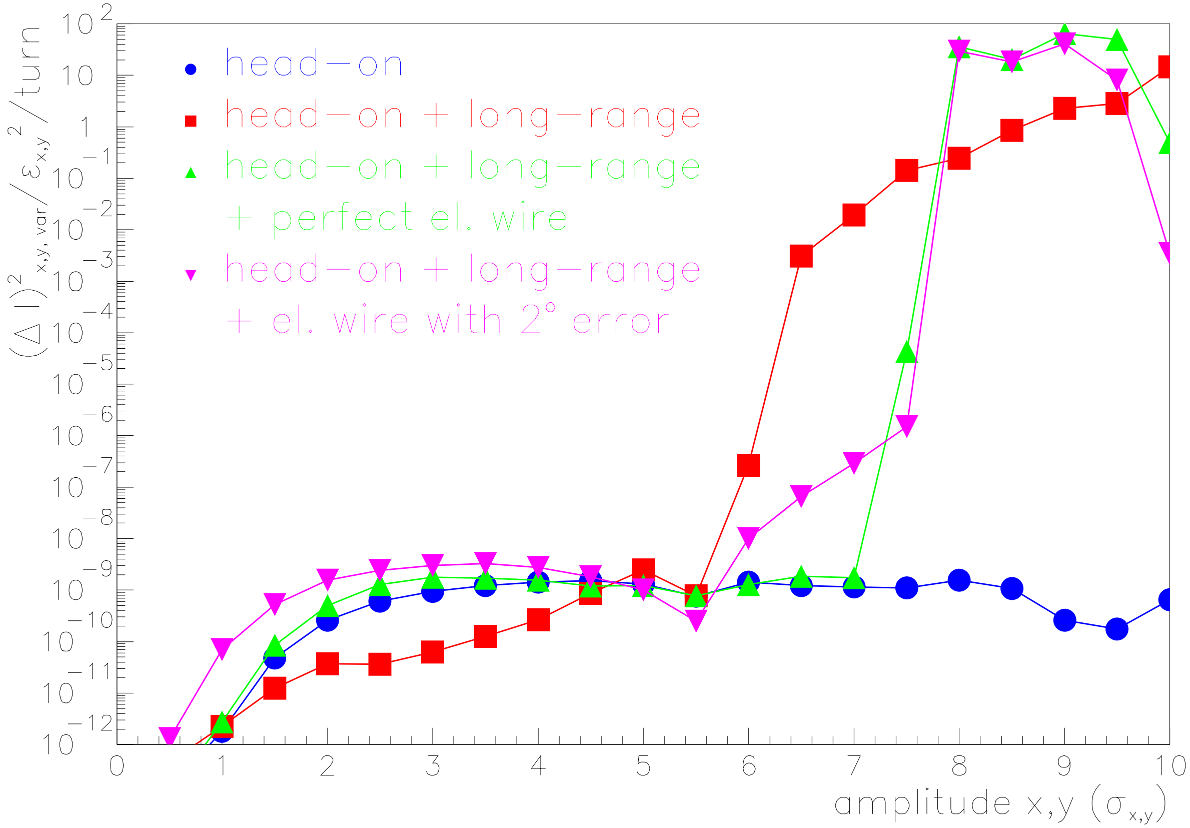

The diffusion per turn as a function of the start amplitude. An electric wire increases the diffusive aperture by about 2σ, even with strength error.

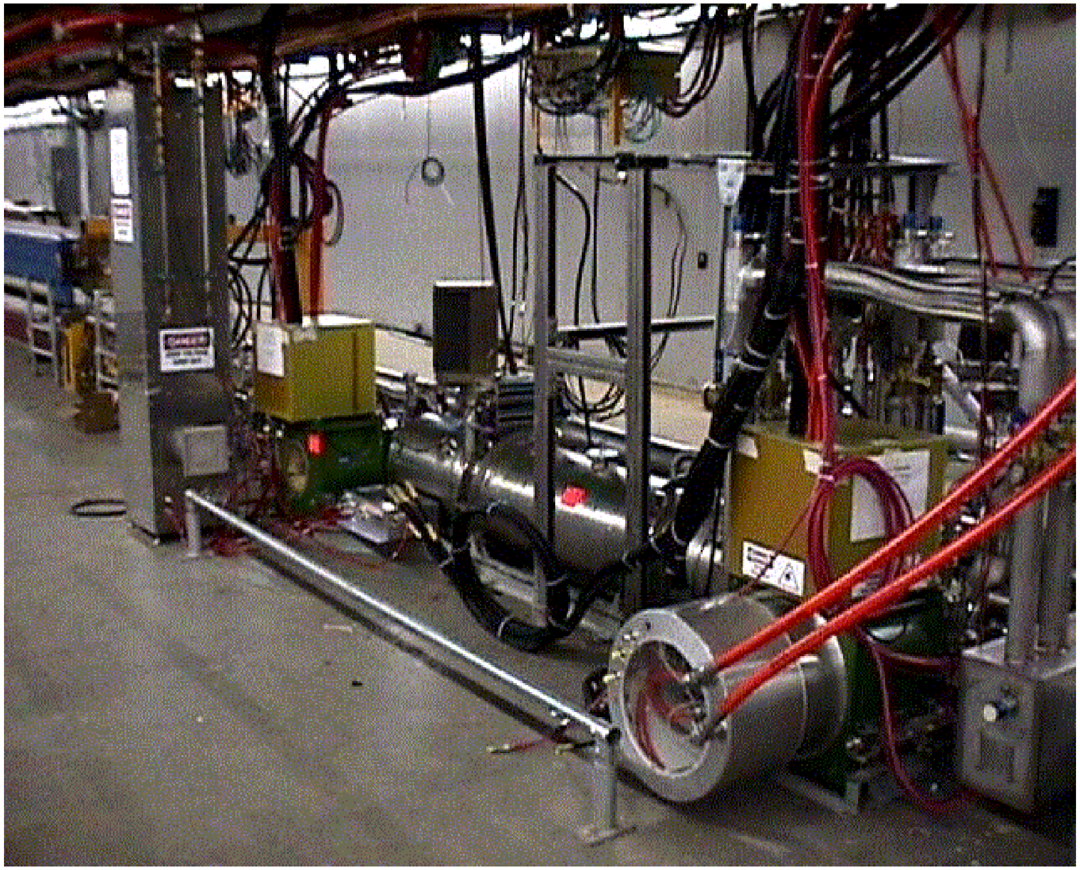

Complementary approach: Tevatron electron lens for beam-beam tune-shift compensation [Courtesy V. Shiltsev, 2001].

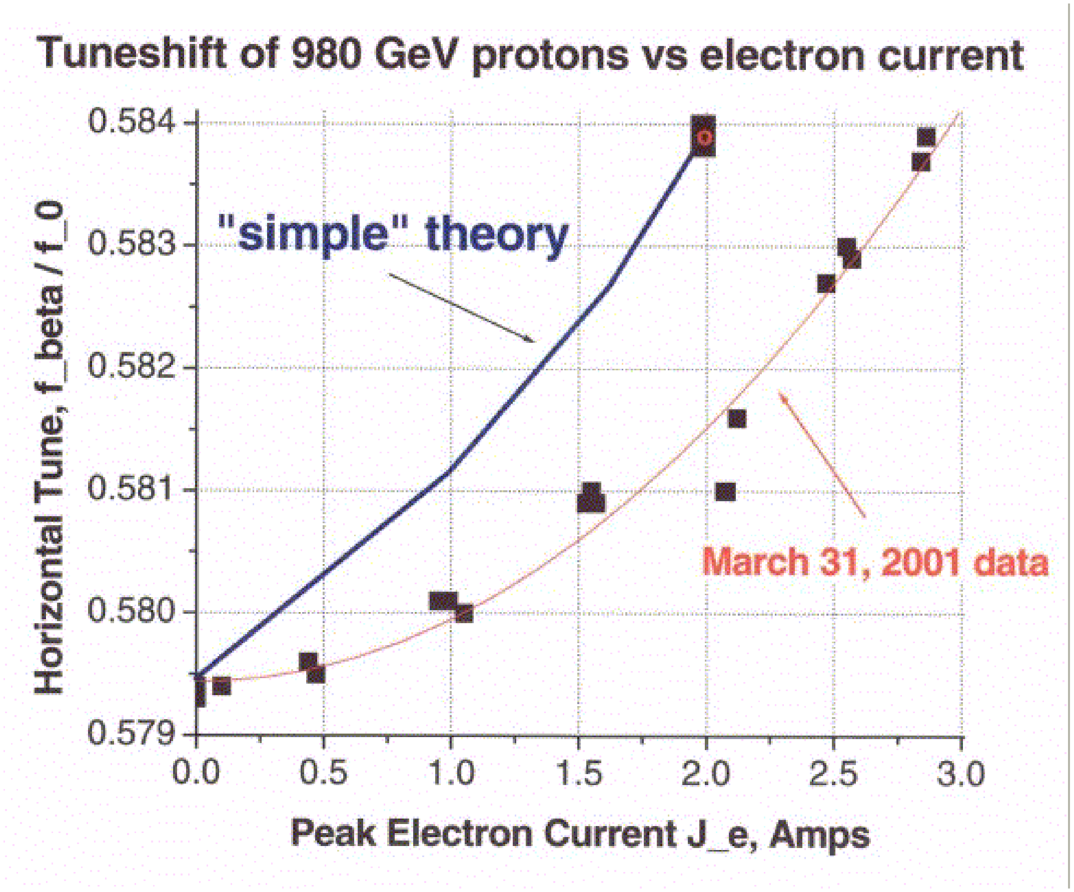

Tevatron proton tune shift as a function of electron current [Courtesy V. Shiltsev, 2001].

Strong-Strong Beam-Beam Effects at LHC

Two colliding bunches → two coherent modes: σ mode (in phase oscillation), and π mode (out-of phase). Frequency of σ mode = unperturbed betatron tune; frequency of the π mode is shifted downwards.

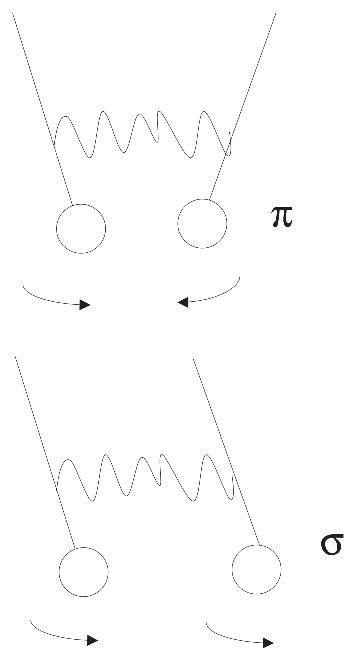

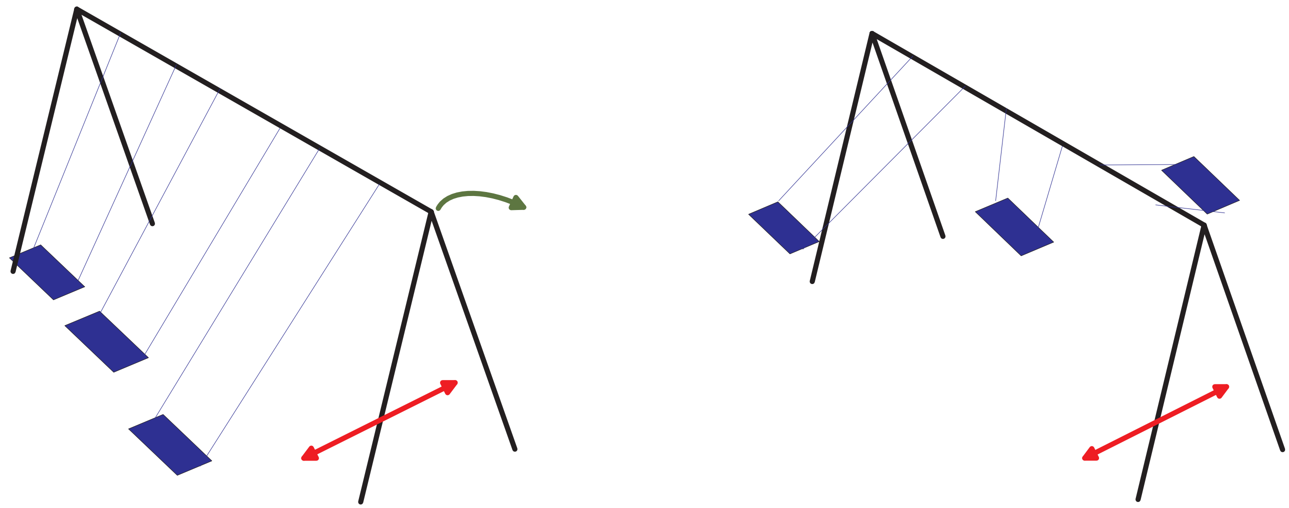

Different oscillation frequencies of individual particles tend to stabilize the coherent beam motion against excitation frequencies within the frequency spread. This is called **Landau damping**.

driven particle motion $\ddot{x} + \omega^2 x = A e^{-i\Omega t}$; beam centroid response: $< x >= \frac{A}{2\bar{\omega}} e^{-i\Omega t} \int d\omega \frac{\rho(\omega)}{\omega - \Omega - i\epsilon}$ $(\epsilon \longrightarrow 0^+)$.

Prediction: coherent π mode in LHC will not be Landau damped! $|(N_1 - N_2)/N_2| < 40\% \quad \rightarrow \quad Q_\sigma - Q_\pi > \xi$ (coherent tune shift > incoherent tune spread) (Alexahin, Yokoya).

De-Stabilizing effect of long-range collisions?

	SPS	TeV-II	LHC
intensity ratio N_1/N_2	2	$9 \rightarrow 2$	1

Simulation studies (M. Zorzano) support predictions, and also indicate that long-range collisions will not stabilize the π mode.

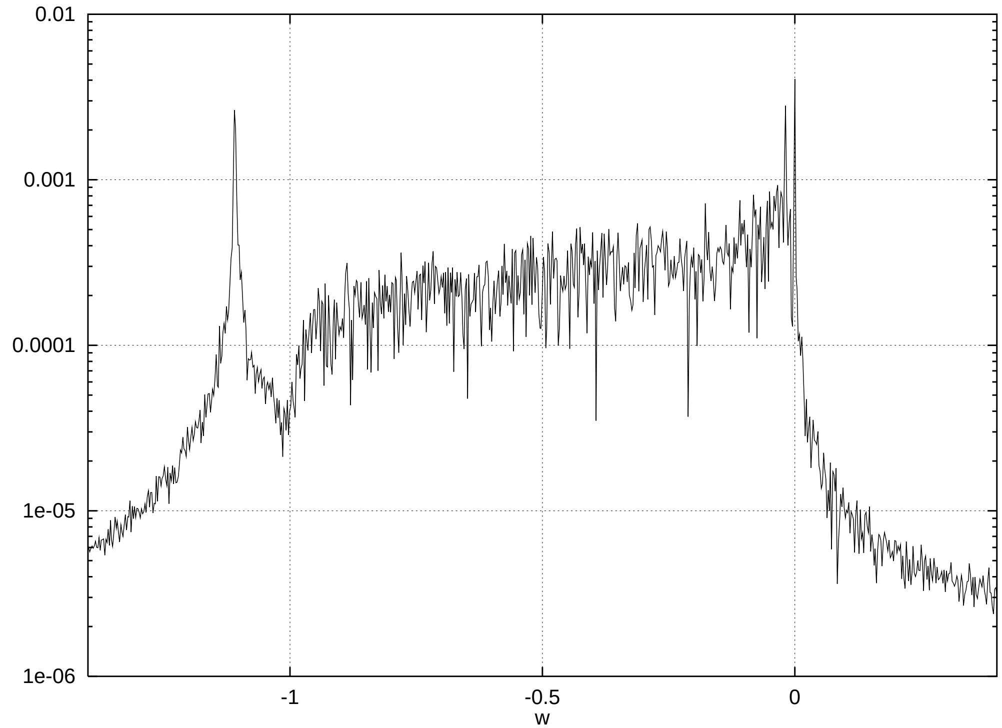

Simulation of coherent modes (M. Zorzano): frequency spectrum of the bunch centroid motion; horizontal axis $w = (\nu - Q)/\xi$. The π- and σ- oscillation modes are clearly visible.

Possible cure: separate the tunes in the two rings! (Hofmann). Simulations suggest that Landau damping may be restored, if the tune split is larger than the beam-beam tune shift .

However, at alternative asymmetric working points coherent resonances may be encountered (Alexahin, Herr, Zorzano)

Both theory and simulations rely on various approximations and assumptions. Experimental studies of the π mode stability in LEP (done) and at RHIC (planned).

Various Single-Beam Collective Effects...

- Coherent Synchrotron Tune Shift; loss of Landau damping requires controlled emittance blow up
- Longitudinal Microwave Instability; safely stable.
- Transverse Mode Coupling; threshold $N_b^{\rm thr} \approx 5.9 \times 10^{11}$ at injection.
- Resistive Wall Instability; nominal LHC: $\tau \approx 30$ ms (300 turns); double bunches and ultimate bunch population: $\tau \approx 10$ ms (100 turns).
- Tune Shift Variation for Partially Filled Ring due to ac magnetic field leakage and finite resistive wall (small effect - J. Gareyte).
- Incoherent Tune Shift due to Collective Fields; Nominal LHC: $\Delta Q_y \approx 0.02$; higher intensity: $\Delta Q_y \approx 0.07$; Potential problems: (1) a reduction of dynamic aperture (2) resonance crossing of the coherent multi-bunch modes.

Dynamic Aperture at Injection

Nonlinear field errors can destabilize particle motion after 1000s of turns. Error sources:

- persistent currents (eddy currents in the superconductor)
- coil geometry
- current redistribution during ramping

Maximum stable area in phase space: *dynamic aperture*

Approach:

- computer simulations or particle motion over 10^6 turns
- experimental comparisons at SPS and HERA
- require 12σ aperture to be sure actual aperture $> 6\sigma$

Persistent Currents - I_{min}

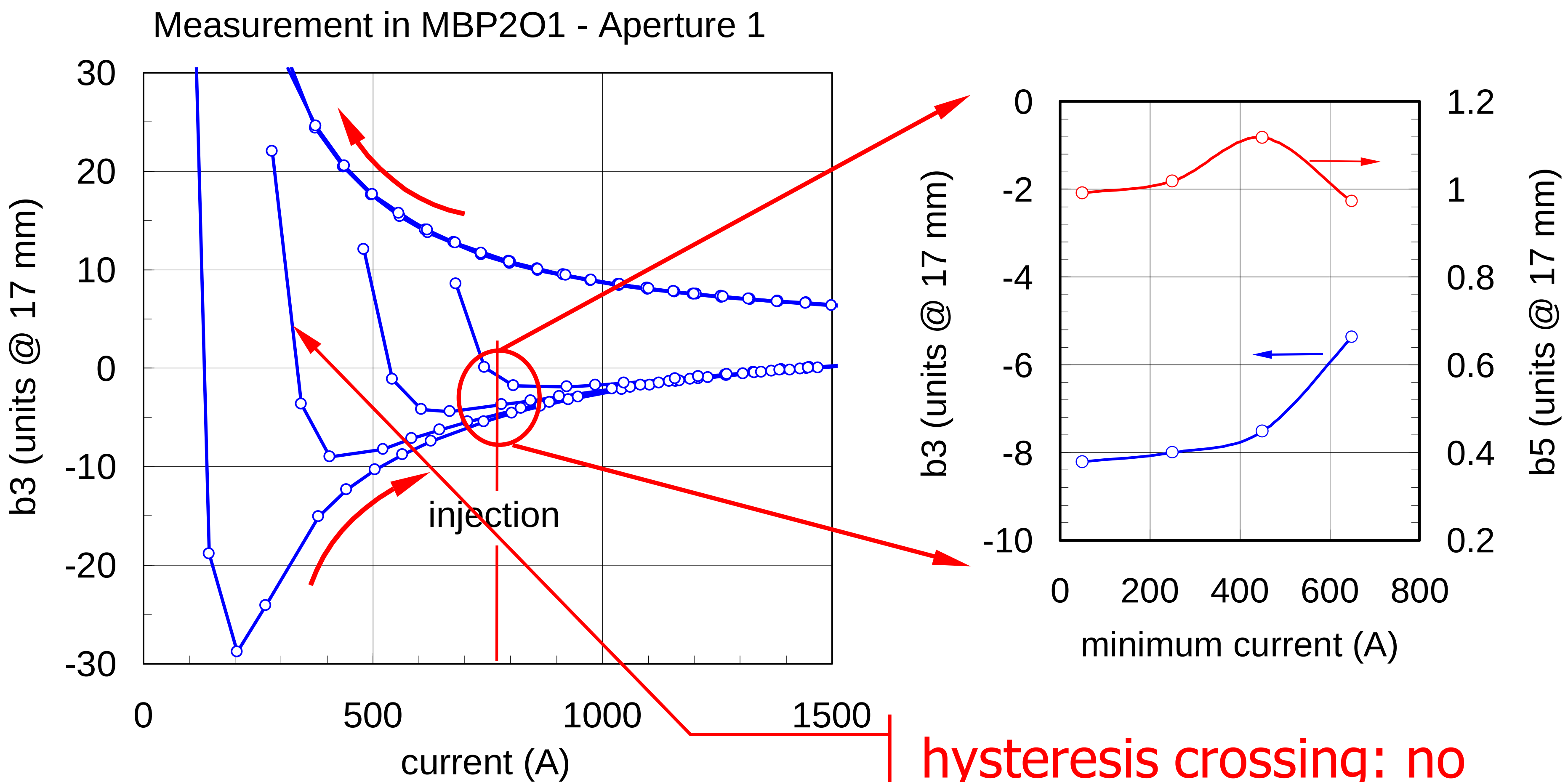

hysteresis crossing: no overshoot possible !

Decay and SB

LHC operation cycle

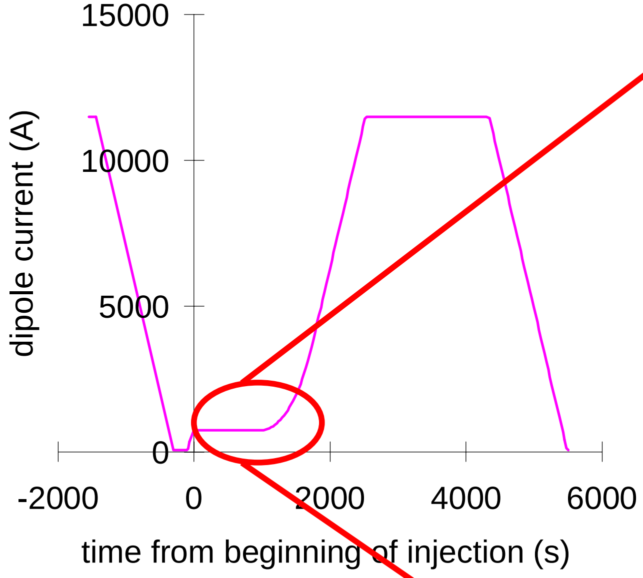

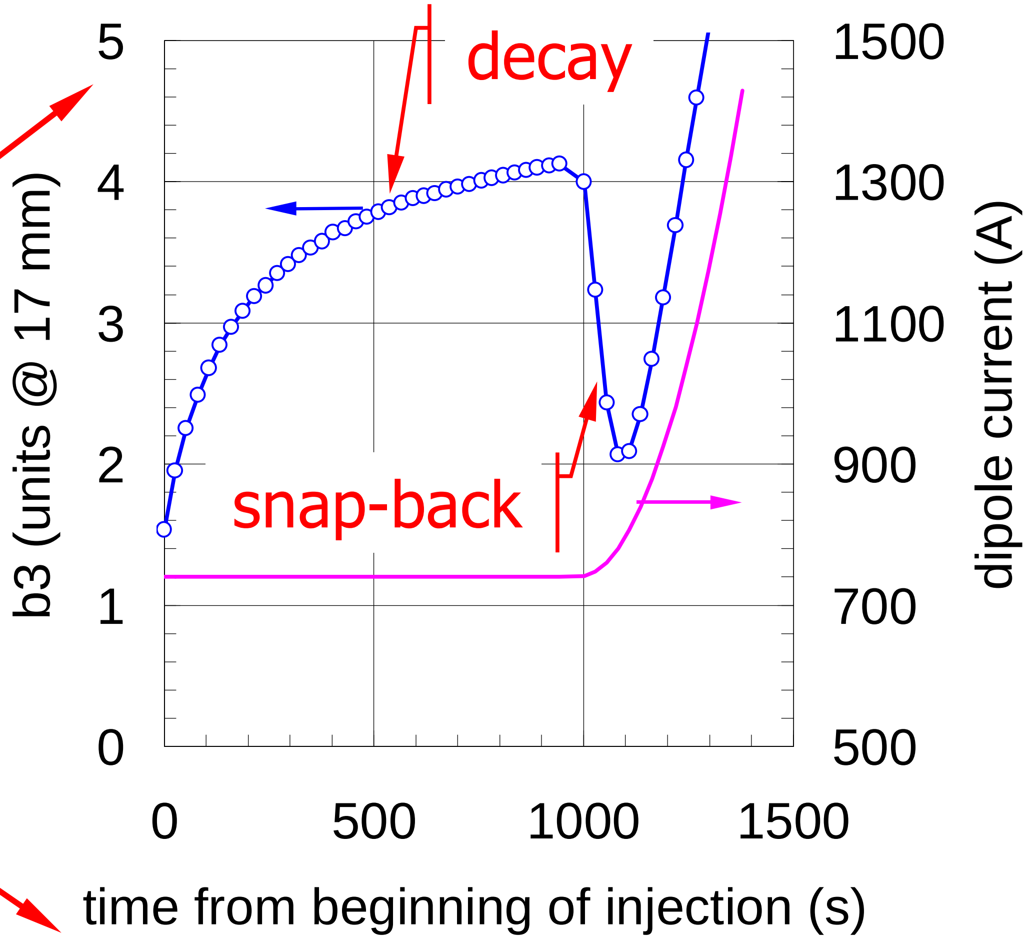

Measurements performed using a prototype of LHC digital controller (SL-PO)

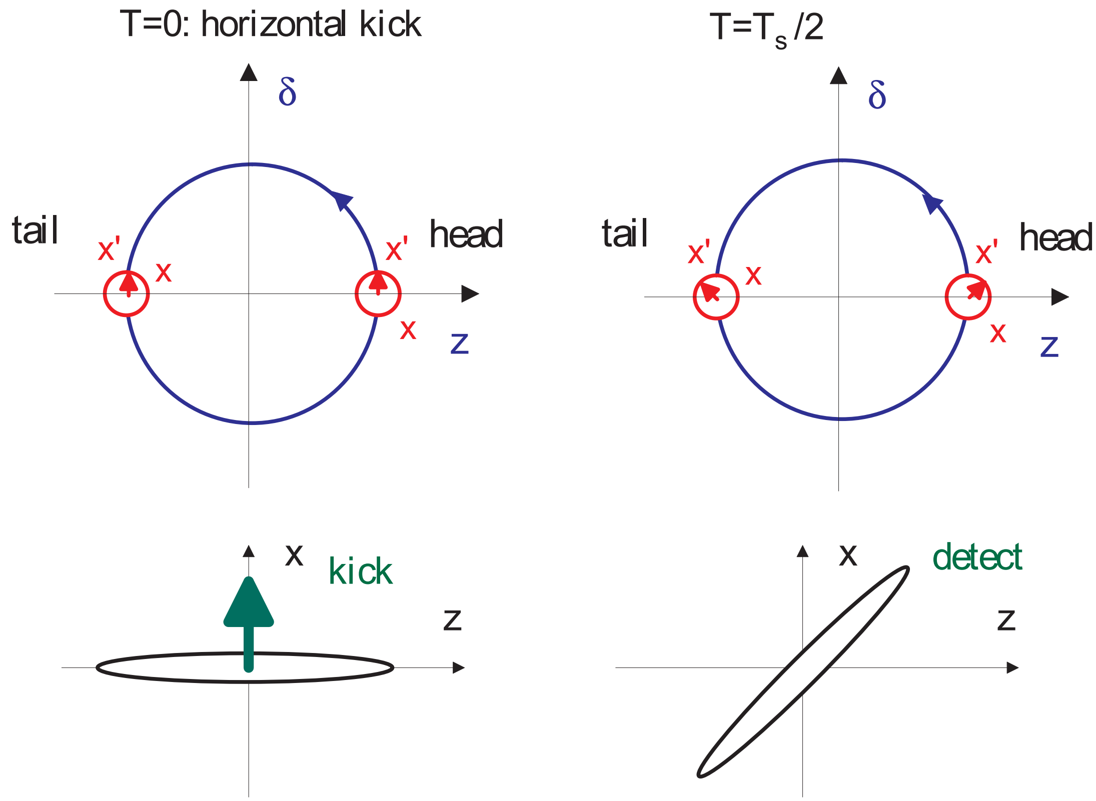

Principle of chromaticity measurement via head-tail phase shift.

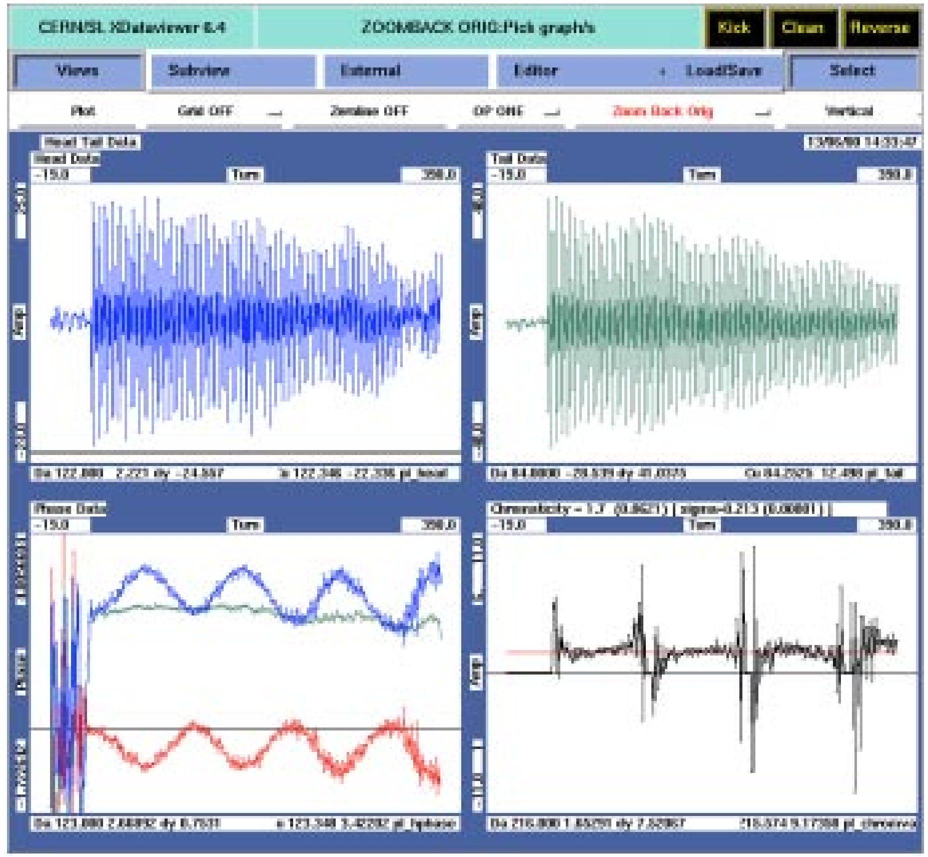

Chromaticity measurement via head-tail phase shift in the SPS.

$$\xi_{x,y} = -\eta \Delta\phi(n) / \left[Q_{x,y} \omega_0 \Delta\tau (\cos(2\pi n Q_s) - 1) \right].$$

Top: raw head and tail oscillations, bottom left: $\Delta\phi$ (red), bottom right: chromaticity. (Courtesy R. Jones, 2000.)

Power Converter Tolerances for LHC

Circuit Type	Nominal Current (A)	Current Polarity	One Year Accuracy (ppm of Inominal)	One day Reproducibility (ppm of Inominal)	1/2 hour Stability (ppm of Inominal)	Resolution (ppm of Inominal)
Main Bends, Main Quads	13000	Unipolar	± 50 ± 20 with calibration	± 5	± 3	1
Inner triplet	8000/ 6000	Unipolar	± 100 ± 20 with calibration?	± 20	± 10	15
Dispersion suppressor	6000	Unipolar	± 70	± 10	± 5	15
Insertion quadrupoles	6000	Unipolar	± 70	± 10	± 5	15
Separators (D1,D2,D3,D4)	6000	Unipolar	± 70	± 10	± 5	15
Trim quadrupoles	600	Bipolar	± 200	± 50	± 10	30
SSS correctors	600	Bipolar	± 200	± 50	± 10	30
Spool pieces	600	Bipolar	± 200	± 50	± 10	30
Orbit correctors	120/60	Bipolar	± 1000	± 100	± 50	30

Precision

Control

Results of Resolution Test with the Prototype Digital Controller

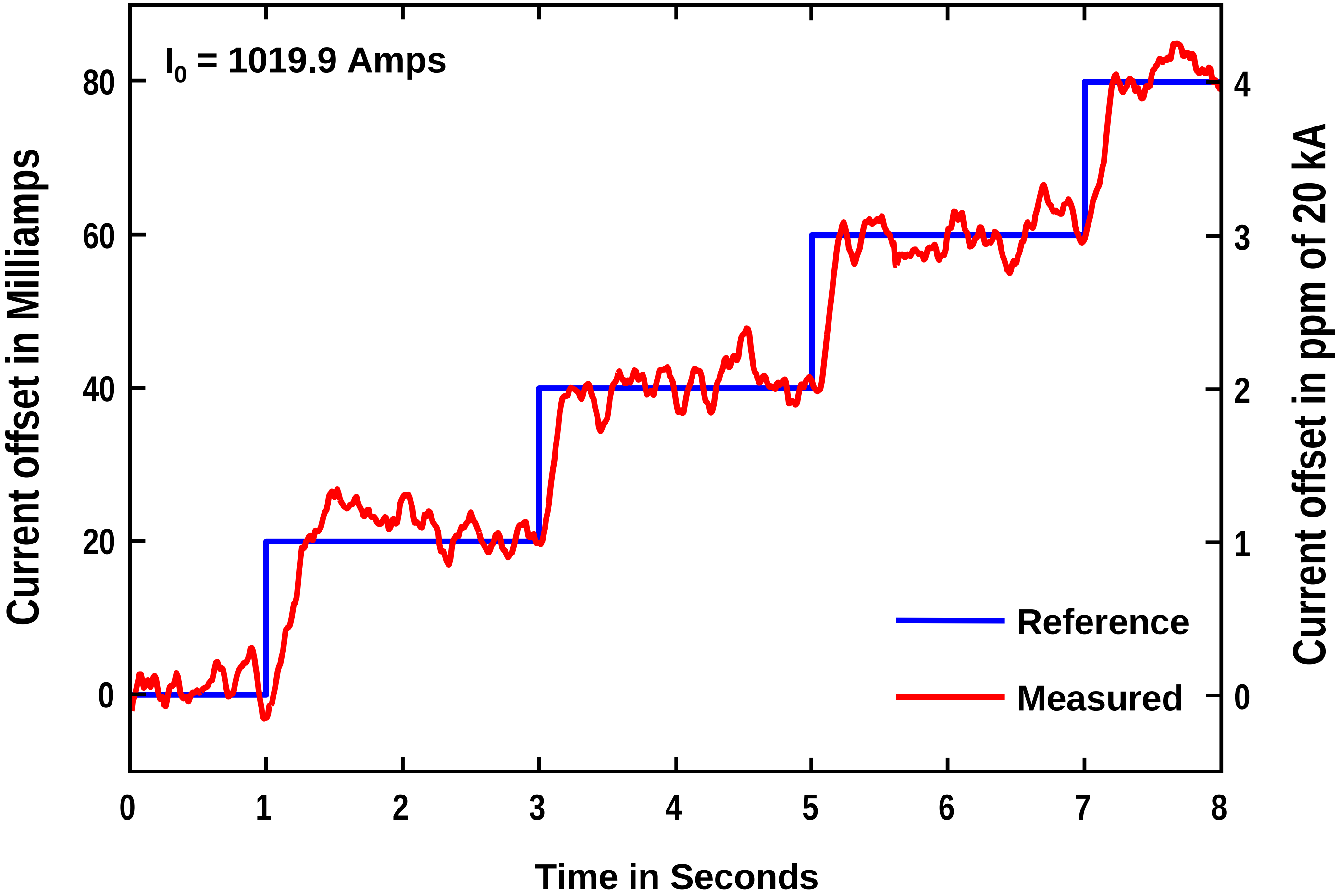

Phase Space Distortions

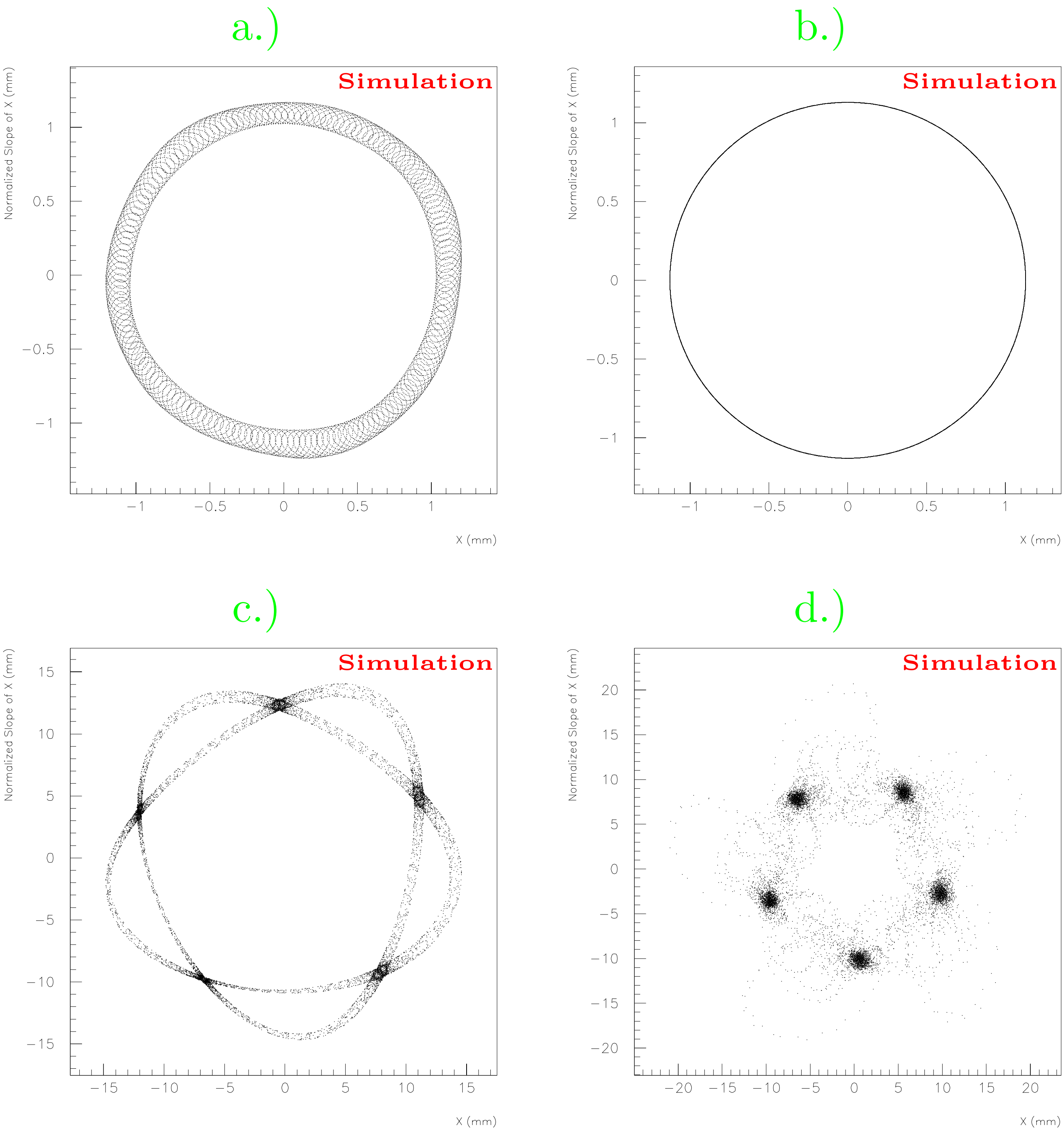

Example Spectrum for the SPS

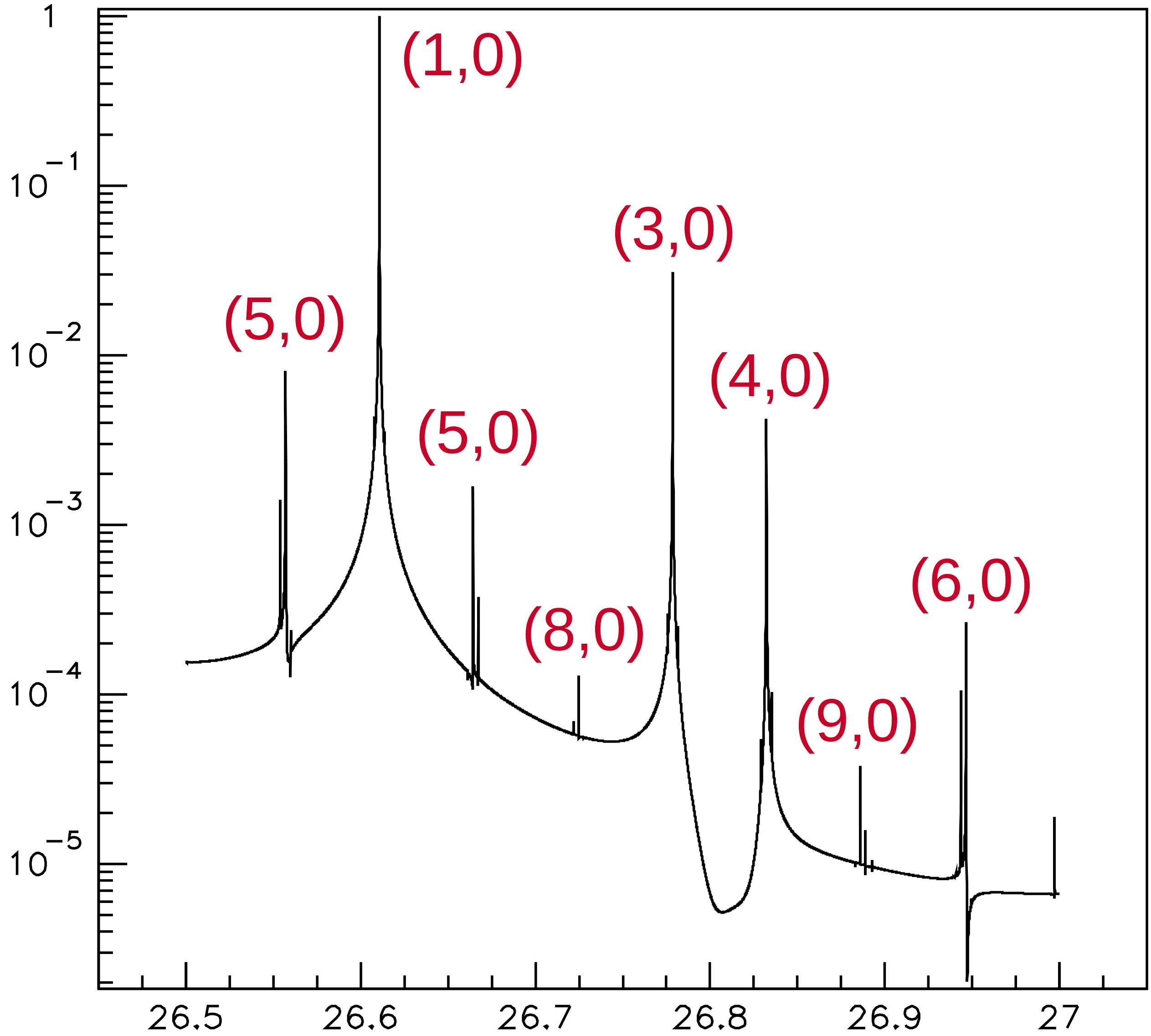

Detuning SPS 120GeV

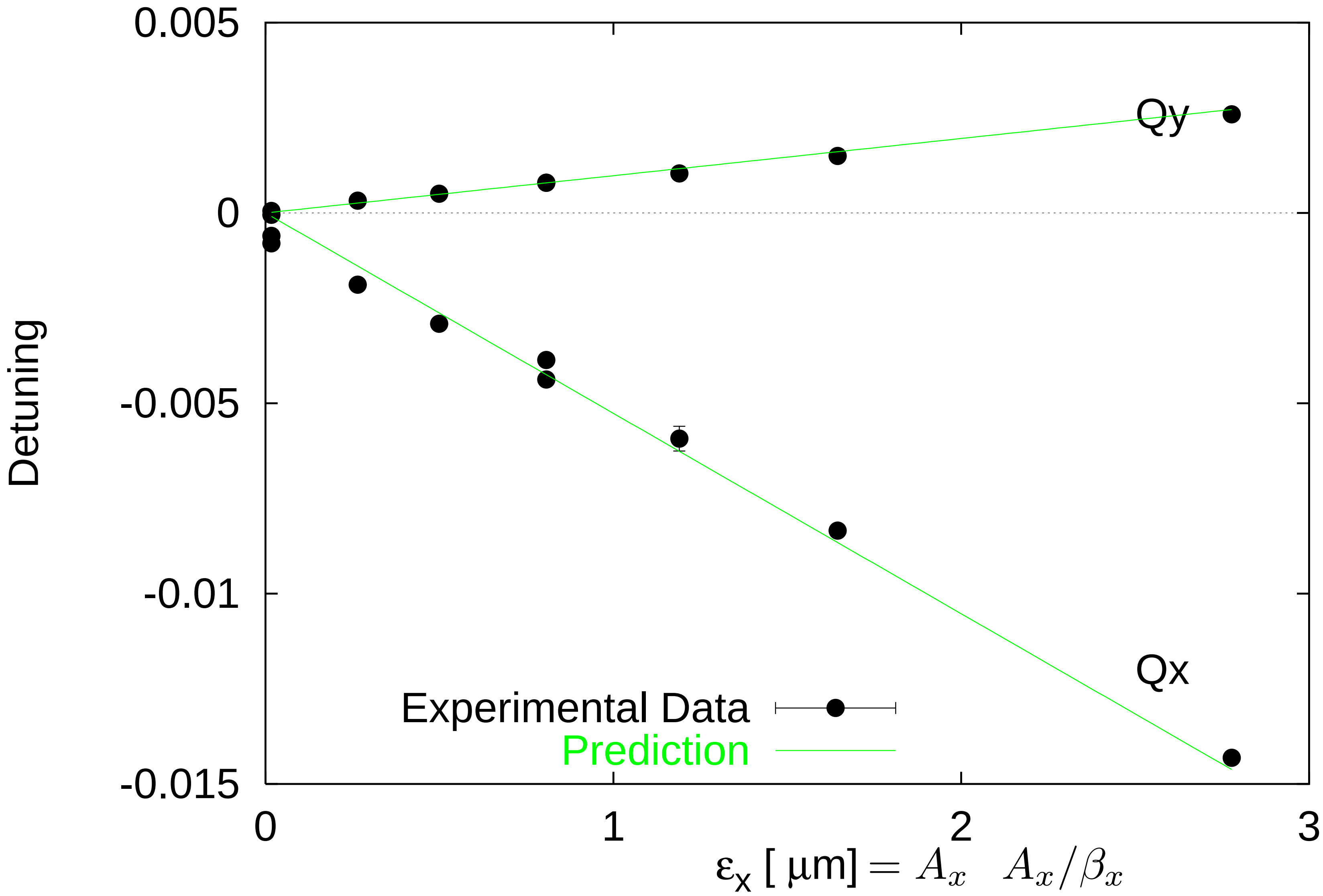

3,0 , 1,0 esonances 120GeV

According to the rule these are the (-2,0), (2,0) spectral lines.

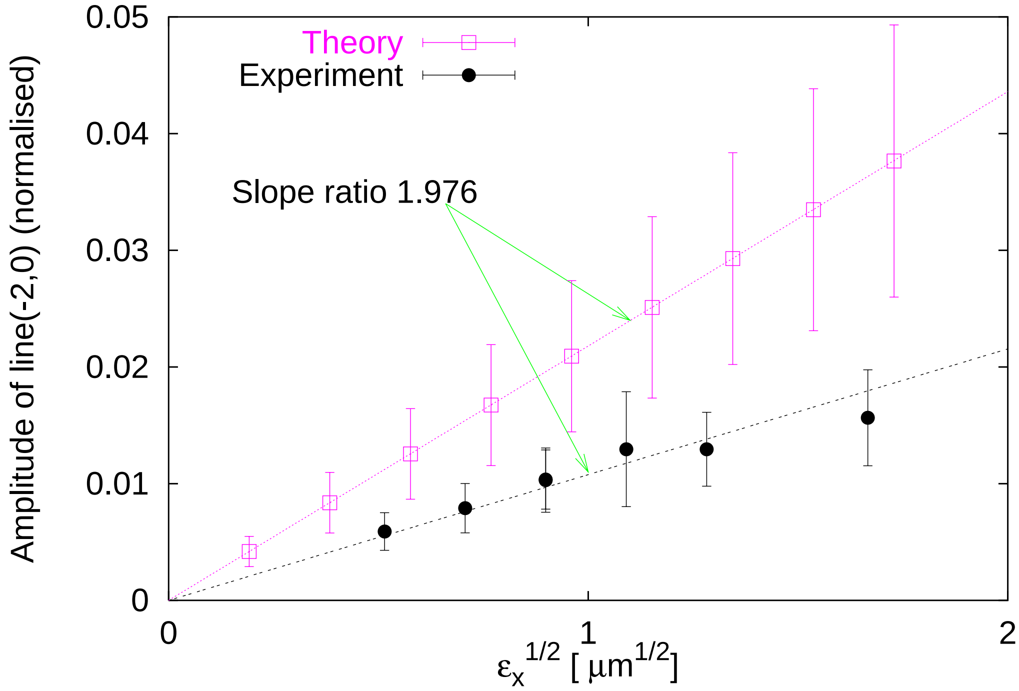

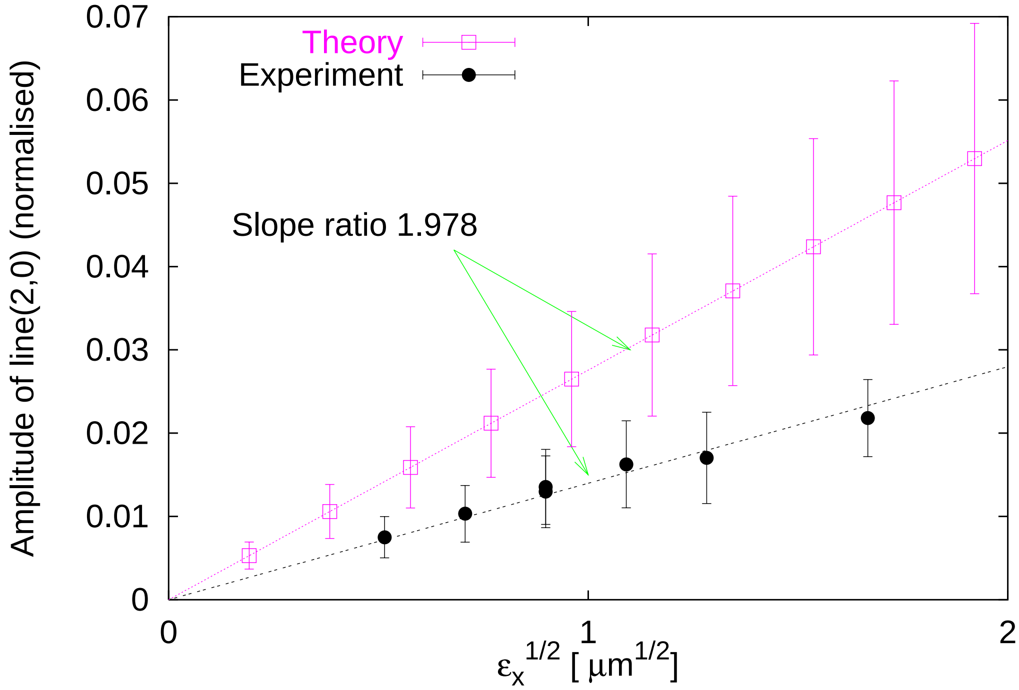

Localisation of Multipoles SPS 120GeV

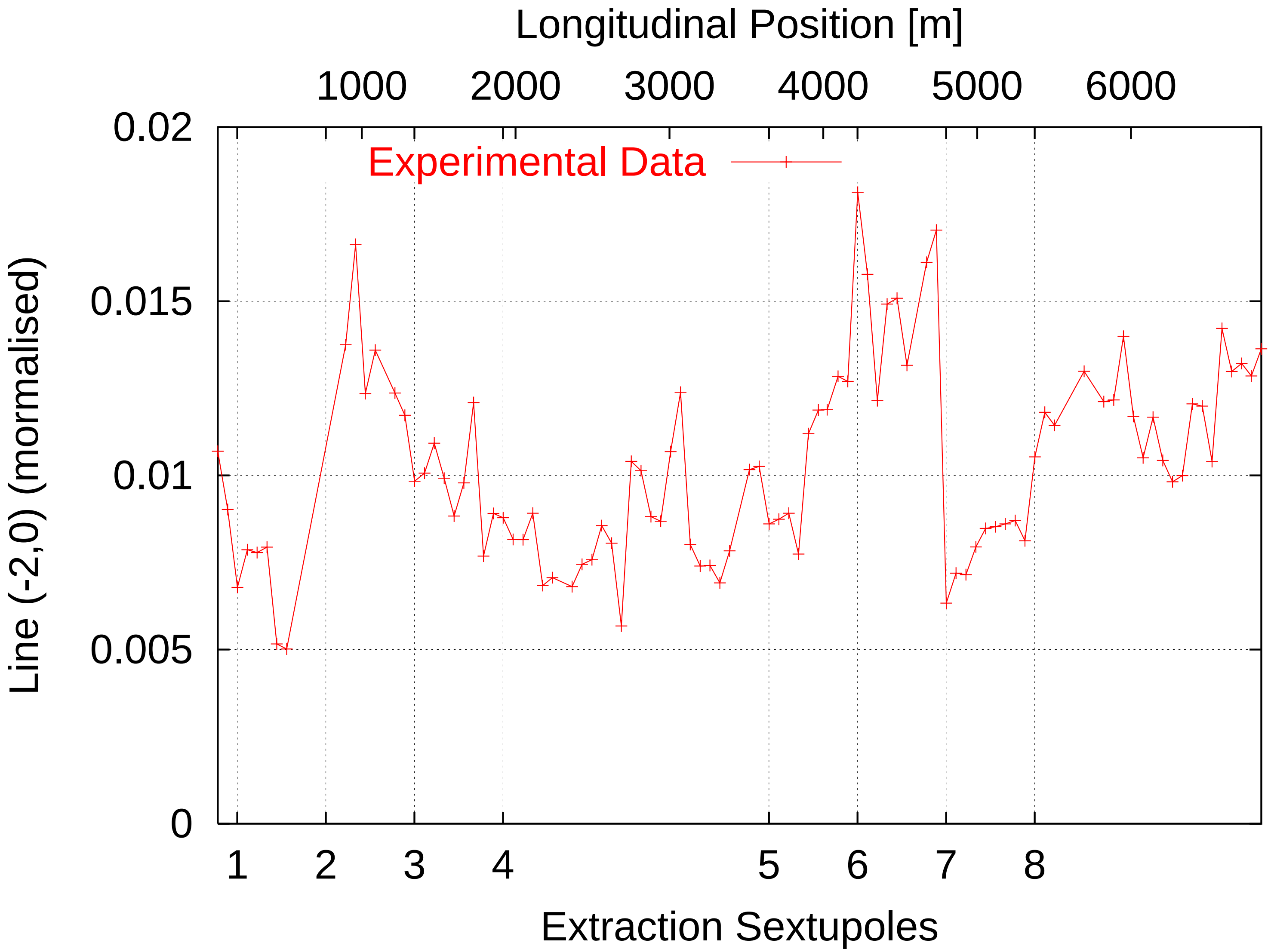

Heat Load inside the Cold Magnets

4 Sources

- lost beam particles (scattered at collision point or at residual gas nuclei; or on unstable trajectory diffusing outwards) $\rightarrow$ collimation $\rightarrow$ cooling with superfluid helium at 1.9 K
- synchrotron radiation: at $N_b \approx 1.6 \times 10^{11}$ about 0.27 W/m $\rightarrow$ beam screen
- image currents ; at $N_b \approx 1.6 \times 10^{11}$ about 0.46 W/m $\rightarrow$ beam screen with copper coating
- electron cloud; residual cooling capacity at $N_b \approx 1.6 \times 10^{11}$ must stay below 0.56 W/m!

Quench Limits:

$\Delta T = 7K$ at injection, and $\Delta T = 1K$ at top energy

Loss mechanisms:

- injection errors (few turns)
- protons outside of the rf bucket: 'flash' at start of ramp ($\sim$1 s)
- continuous losses in collision

process	exp. losses	quench limit	l_f factor [m]
injection	$\Delta N = 1.25 \times 10^{12}$	$\Delta N_q = 10^9$	1250
ramping	$\Delta N = 9 \times 10^{12}$	$\Delta N_q = 2.5 \times 10^{10}$	360
collision	$\dot{N} = 3 \times 10^9$ s^{-1}	$\dot{N}_q = 6 \times 10^6$ m^{-1}s^{-1}	500

Collimation

2-stage system:

3 primary betatron collimators at 6σ & 1 energy collimator;

each followed by a set of three secondary collimators at 7σ;

collimation inefficiency depends on ring aperture $A_{\rm ring}$;

if $A_{\rm ring} = 8\sigma$: $\eta_{\rm coll} \approx 10^{-4}$;

collimation must be in working position at injection;

dynamic closed orbit stability $< 30\ \mu$m $(1/10\sigma)$

Thermodynamic Considerations

Heat capacities

$$\Delta T = \frac{1}{C} \frac{\Delta U}{\Delta m}$$

Cu at 1.9 K: $C_{Cu} \approx 0.03$ **J/kg/K** $\rightarrow$ premature quenches

superfluid helium at 1.9 K: $C_{He} \approx 4000$ **J/kg/K**

measured helium content in s.c. cable $\sim 4.5\%$

the helium absorbs energy and transports it away from the coils

Refrigeration (Carnot) Efficiency

$$\eta = \frac{T_{\rm cold}}{T_{\rm warm}} \qquad P_{\rm warm} = \frac{P_{\rm cold}}{\eta} = \frac{T_{\rm warm}}{T_{\rm cold}} P_{\rm cold}$$

LHCbeamscreen

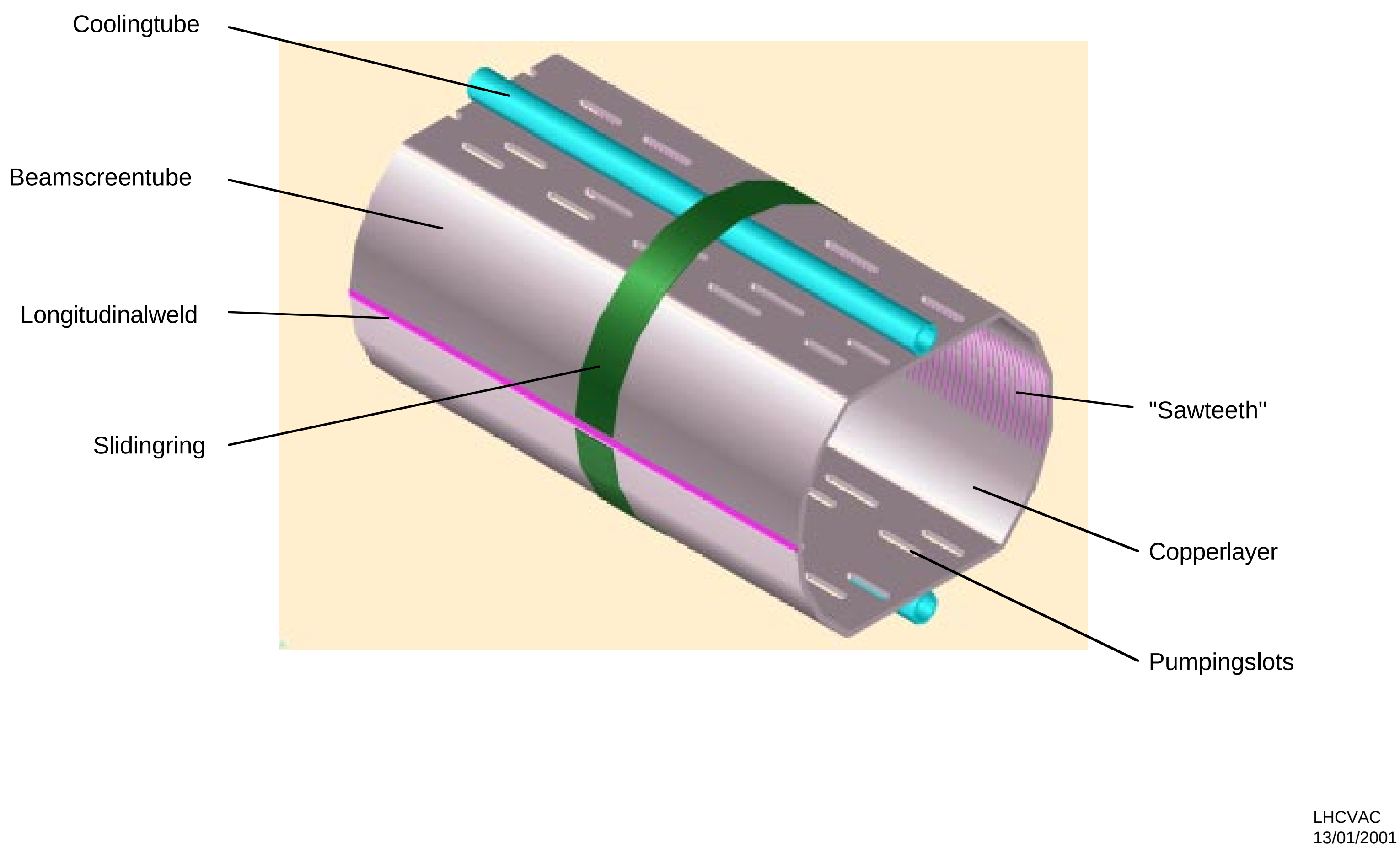

Schematic of LHC beam screen operating at $T \approx$5–20 K. (Ian Collins, 2001).

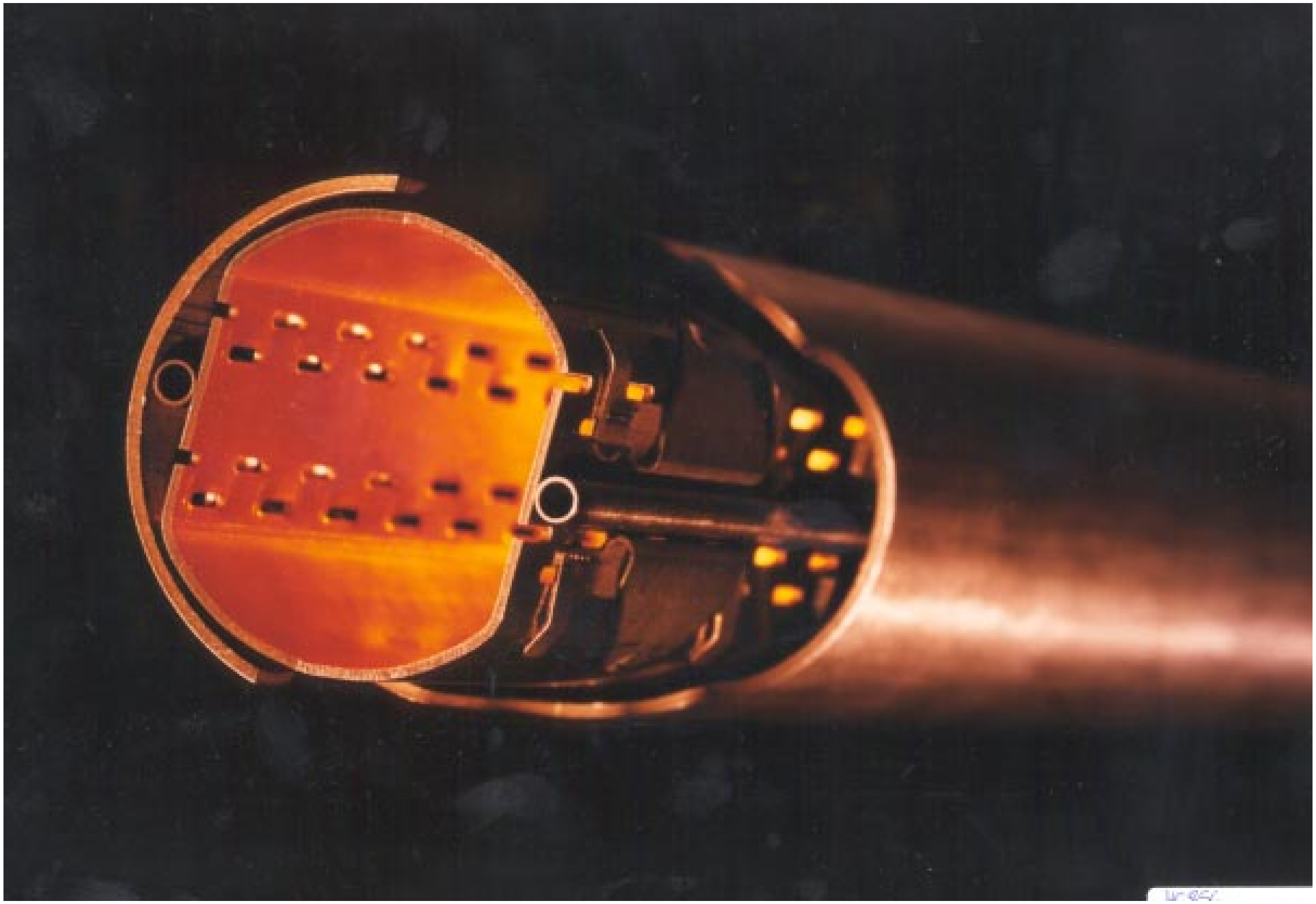

LHC beam screen prototype. (Ian Collins, 2001).

Why Protection?

- Stored magnetic energy= 8*1.3GJ +...
- Beam energy= 0.7 GJ
- Long repair times (if possible at all)
- Long set-up times

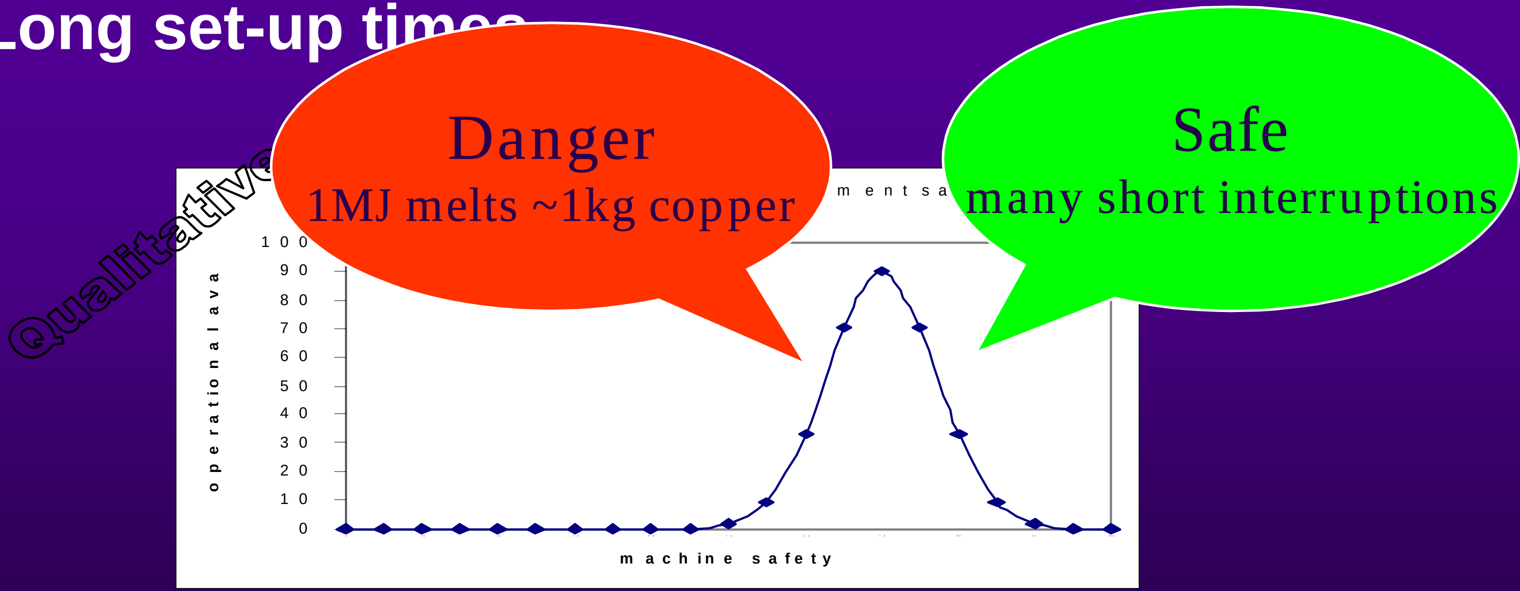

Why Protection?

- **Total stored energy= 11GJ**

at 30 knots

LHC Beam Dump

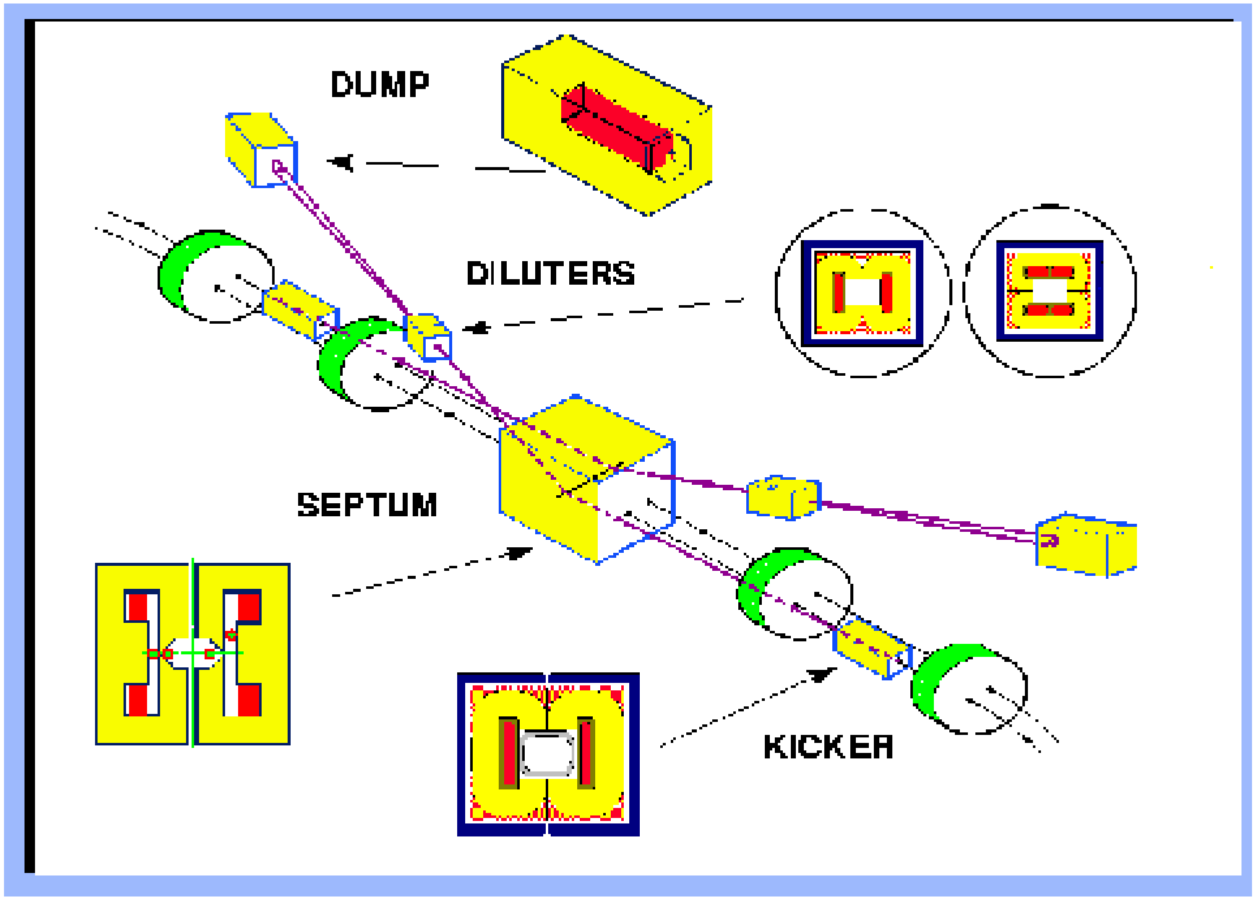

Layout of the LHC beam abort system. (J.M. Zazula et al.)

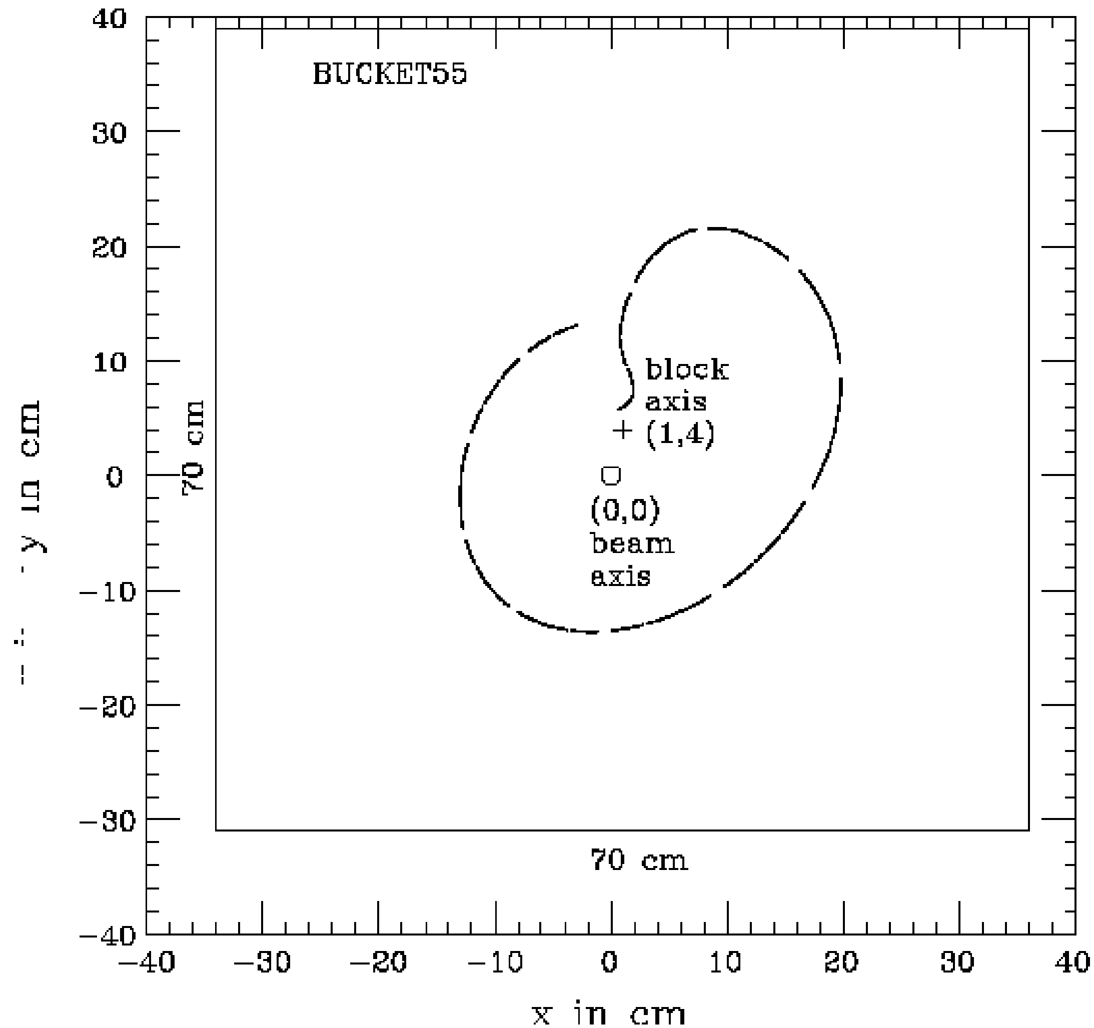

Optimized sweep profile and lateral alignment of the graphite block (J.M. Zazula et al.)

Candidate Materials for Dump (J.M. Zazula et al.)

material	T_{melt} [°C]	T_{max} [°C/bunch]	T_{front} [°C/beam]
Be	1280	75	3520
C	4500	320	3520
Al	660	360	3390
Ti	1670	1800	3250
Fe	1540	2300	3120
Cu	1080	4000	2980

LHC Filling Pattern

bunch-to-bunch spacing 25 ns, total revolution time: 88.924 μs

$$
\begin{aligned}
&(((72 \times b + 8 \times e) \times 3) \quad + \quad 30 \times e) \times 2) \\
&+((72 \times b + 8 \times e) \times 4) \quad + \quad 31 \times e) \times 3) \\
&+((72 \times b + 8 \times e) \times 3) \quad + \quad 30 \times e) \times 3) \\
&\qquad\qquad\qquad\qquad\qquad\qquad +81 \times e)
\end{aligned}
$$

$(\tau_1 = 12$	missing bunches	rise kicker extr. PS)
$\tau_2 = 8$	missing bunches	rise kicker inj. SPS
$\tau_3 = 30,\ 31$	missing bunches	rise kicker inj. LHC
$\tau_4 = 111$	missing bunches	rise kicker extr. LHC

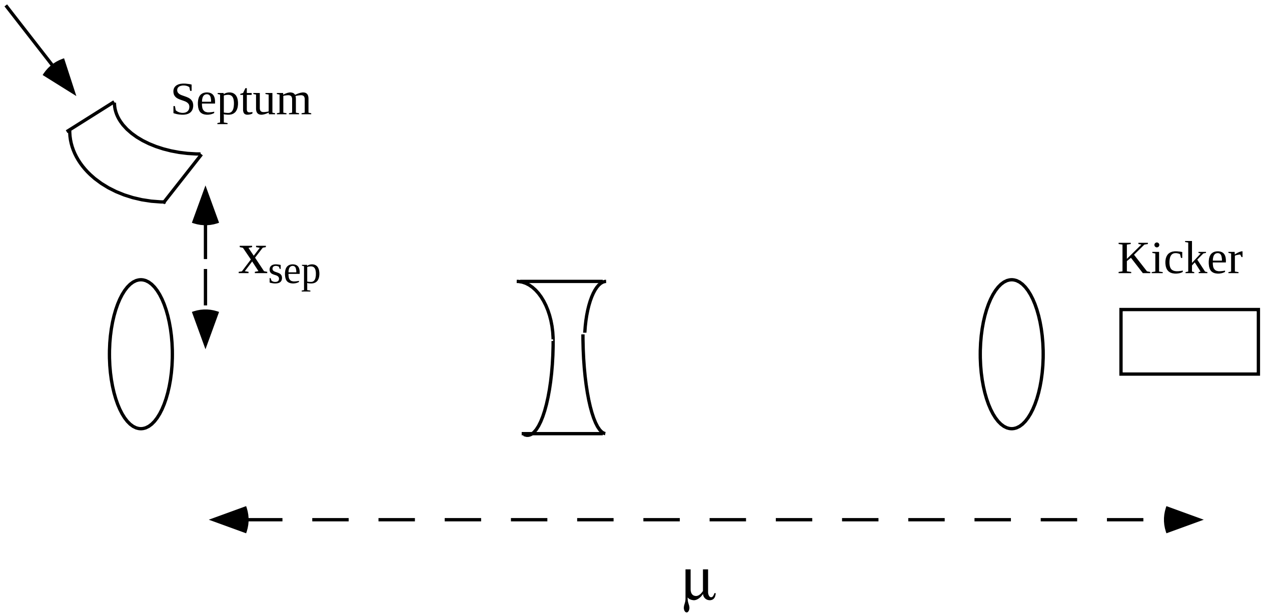

Schematic of injection with septum and kicker magnets

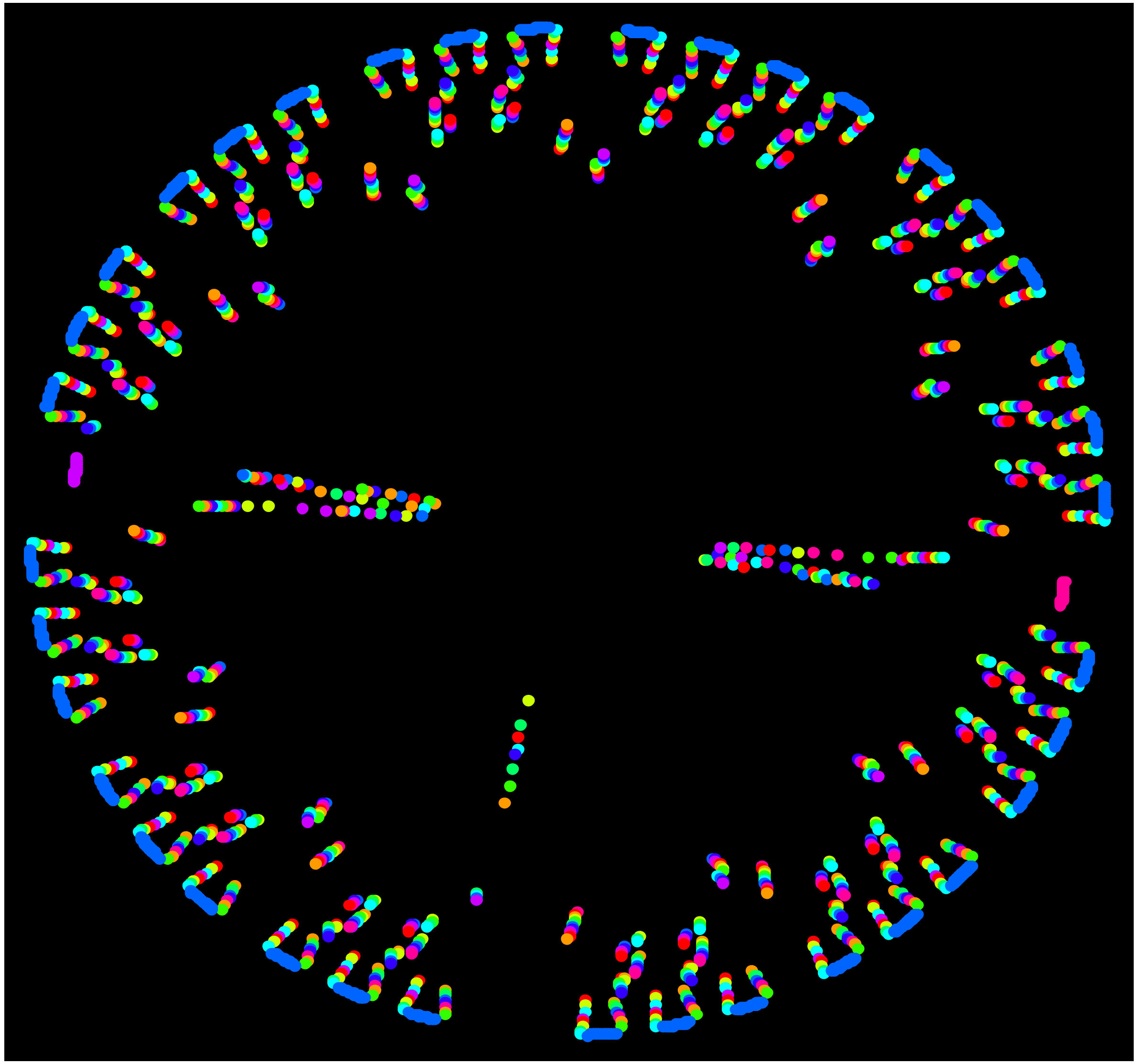

equivalence classes for LHC collision schedule
- graphical representation (J. Jowett)

CERN Accelerators
(not to scale)

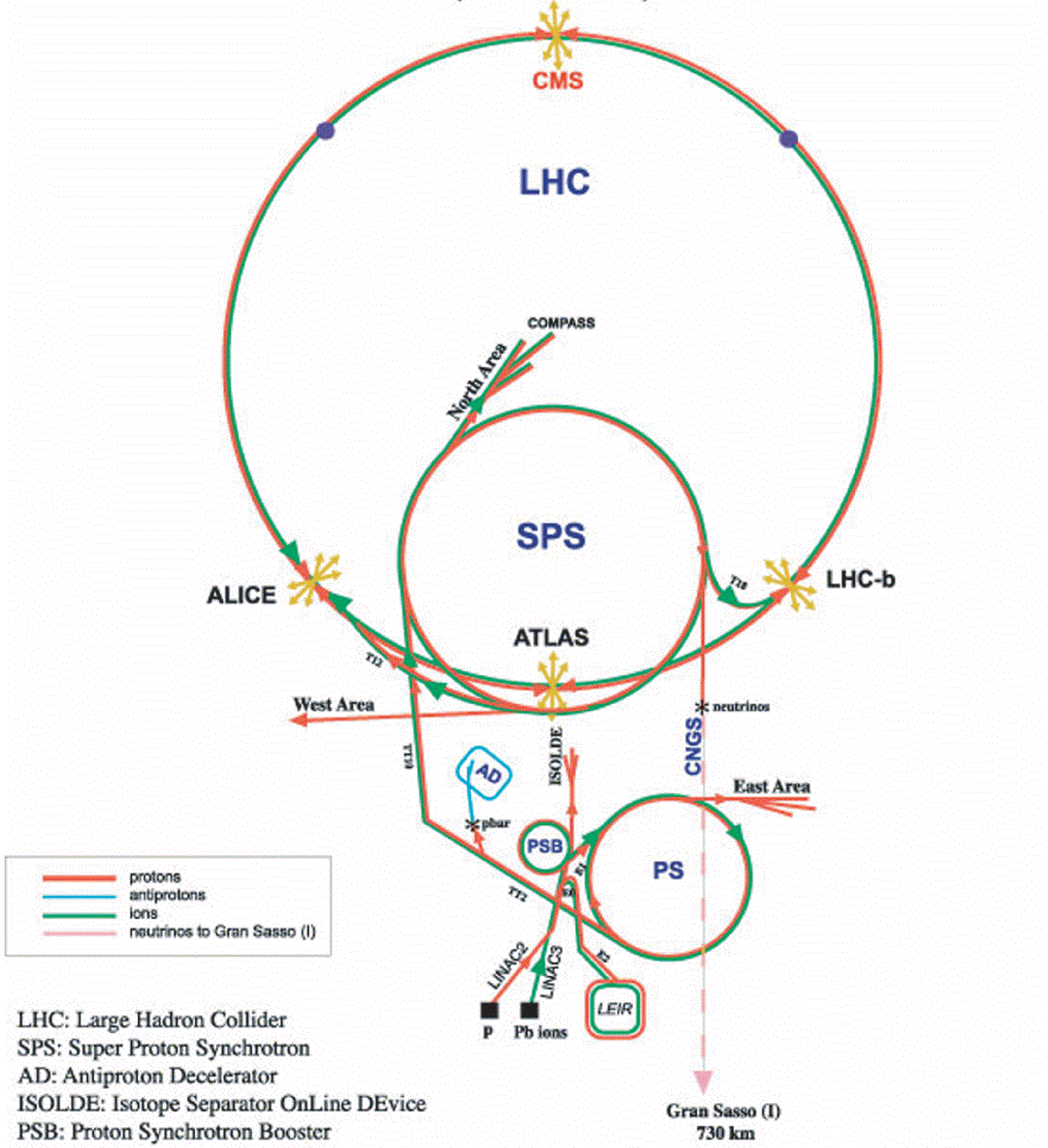

LHC: Large Hadron Collider
SPS: Super Proton Synchrotron
AD: Antiproton Decelerator
ISOLDE: Isotope Separator OnLine DEvice
PSB: Proton Synchrotron Booster
PS: Proton Synchrotron
LINAC: LINear ACcelerator
LEIR: Low Energy Ion Ring
CNGS: Cern Neutrinos to Gran Sasso

Rudolf LEY, PS Division, CERN, 02.09.96
Revised and adapted by Antonella Del Rosso, ETT Div.,
in collaboration with B. Desforges, SL Div., and
D. Manglunki, PS Div. CERN, 23.05.01

LHC (Pre-)Injectors

- 4 PS Boosters
- Proton Synchrotron (PS)
- Super Proton Synchrotron (SPS)

Generating multiple bunches via debunching.

In the past multiple bunches were generated by debunching (rf off) and recapturing in higher-harmonic rf system.

Schematic of phase space evolution during slow debunching.

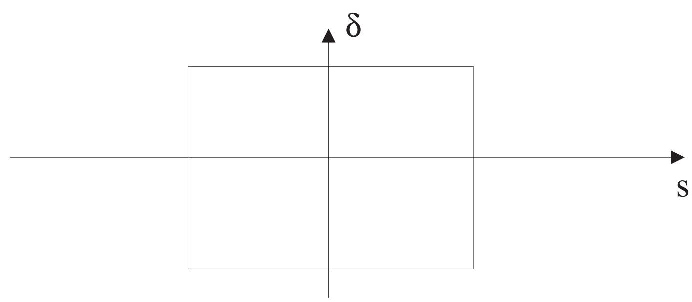

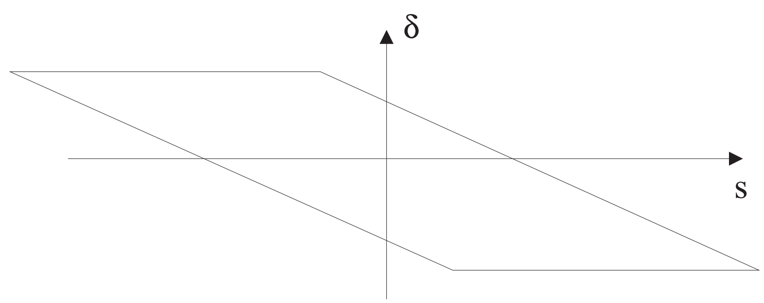

Local μ-wave instability threshold:

$$\left(\frac{dN}{ds}\right)_{\rm thr} \propto \delta_{\rm rms}^2$$

(Boussard criterion). During debunching the density dN/ds and local energy spread $\delta_{\rm rms}$ decrease by the same factor.

$\longrightarrow$ beam becomes unstable, when threshold condition is reached! ($\longrightarrow$ unequal fill patterns, non-reproducibility,...)

Controlled Bunch Splitting for LHC

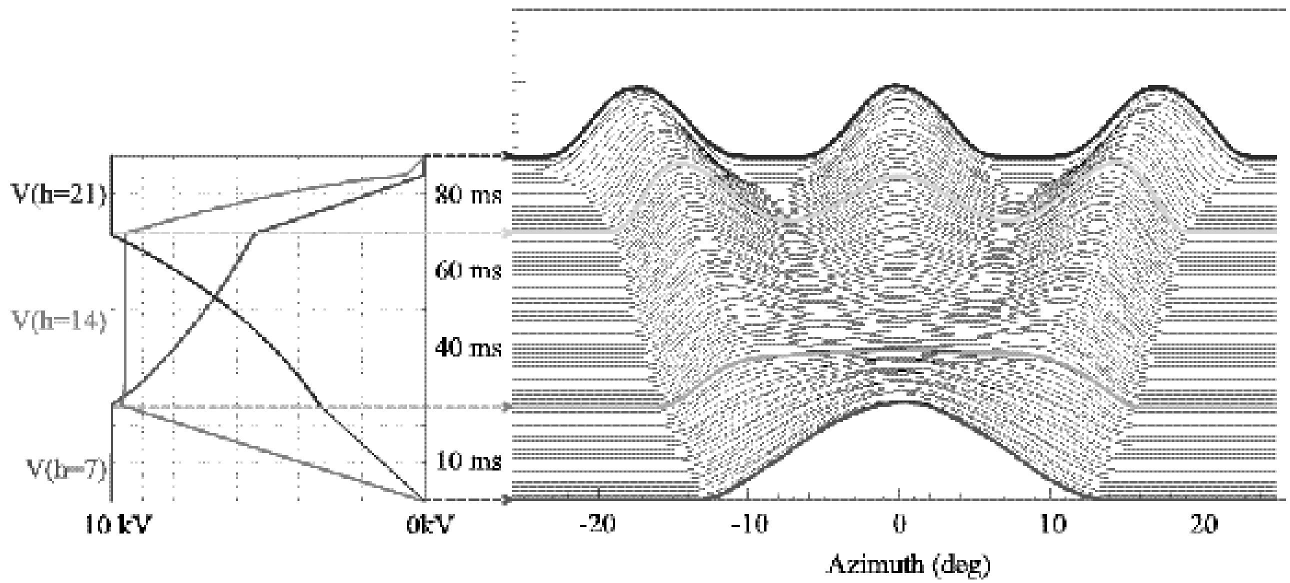

Simulation of bunch splitting in the CERN PS at low energy in preparation for injection into the LHC. (Courtesy R. Garoby, 1999.)

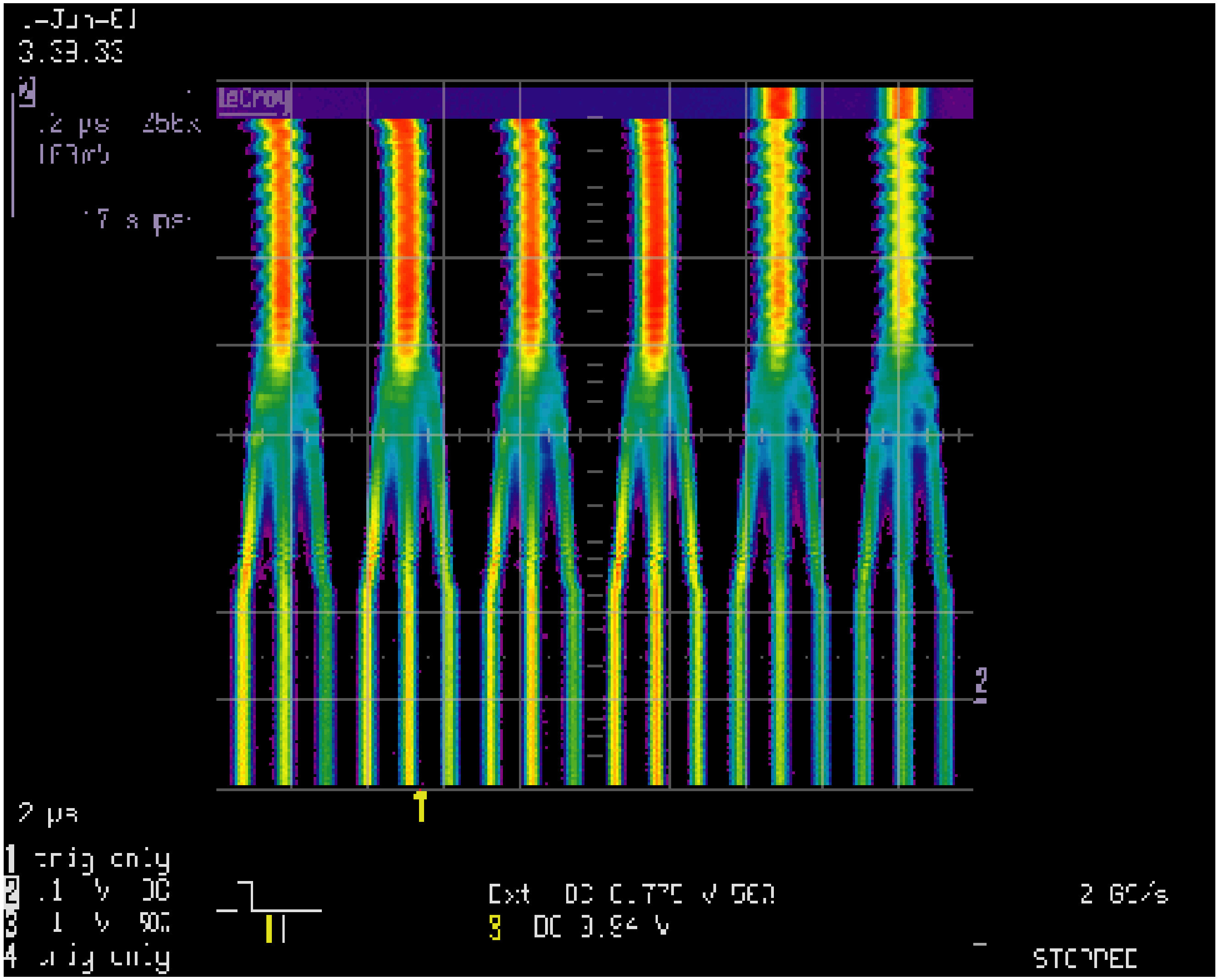

Measured triple bunch splitting in the CERN PS at low energy in preparation for injection into the LHC. (R. Garoby, 2001.)

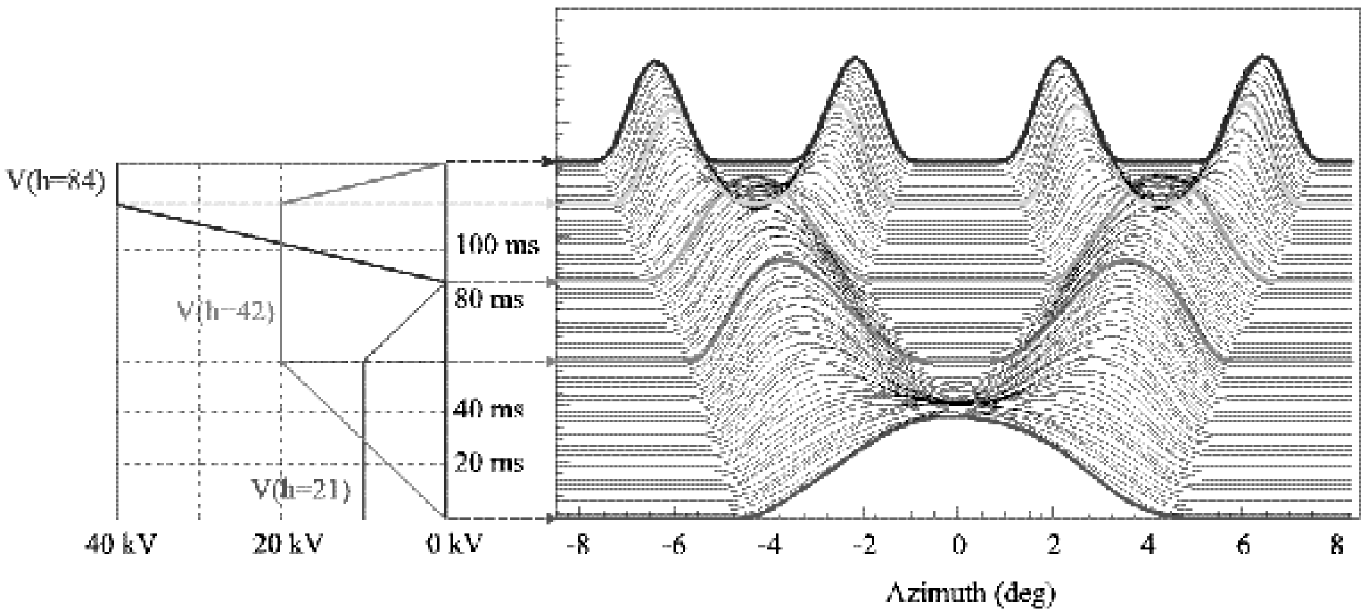

Simulation of further bunch splitting in the CERN PS at high energy (26 GeV/c) in preparation for injection into the LHC. (Courtesy R. Garoby, 1999.)

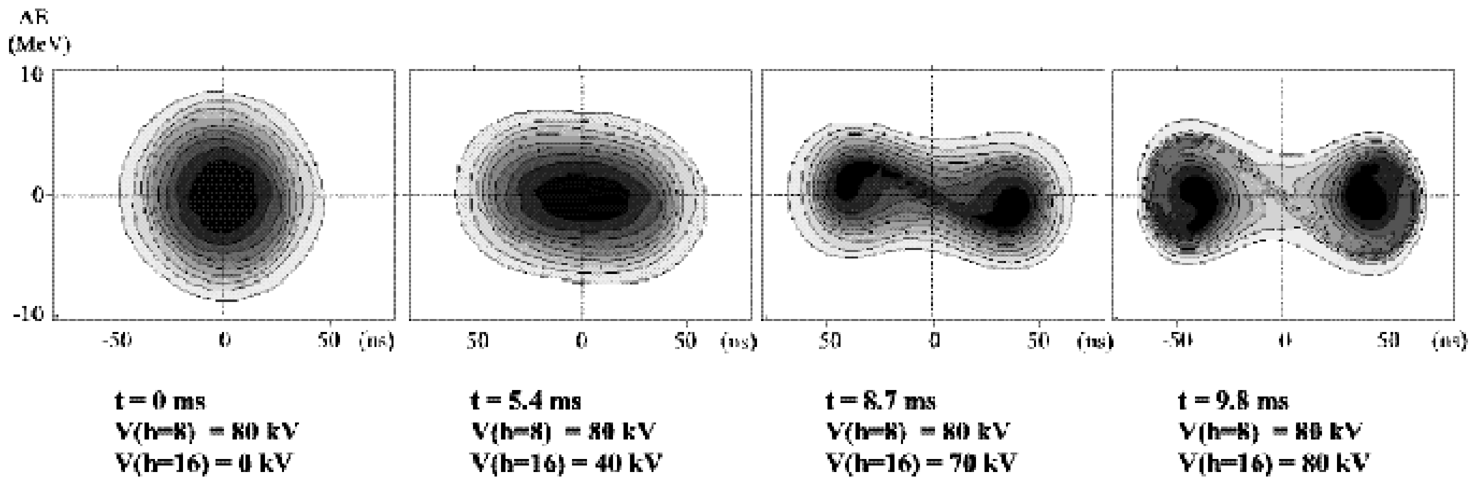

Tomographic measurement of bunch splitting in the CERN PS booster ring after acceleration with 3×10^{12} protons. (Courtesy R. Garoby, 1999.)

Status of the PS for the LHC Nominal Beam

	achieved	nominal
protons per bunch	1.1×10^{11}	1.1×10^{10}
hor. emittance $\gamma\epsilon_x^{1\sigma}$ [μm]	2.5	3
vert. emittance $\gamma\epsilon_y^{1\sigma}$ [μm]	2.5	3
long. emittance $\epsilon_l^{2\sigma}$ [eVs]	0.35	0.35
total bunch length l_b [ns]	≤ 4	4
momentum spread $2\sigma_p/p$ [10^{-3}]	2.2	2.2

SPS Transverse Impedance

18 MΩ/m	D. Boussard, J. Gareyte 1980
47.7 MΩ/m	T. Linnecar, W. Scandale 1984
13 MΩ/m	L. Vos 1986
26.8 MΩ/m	D. Brandt et al, 1988
(23 ± 2) MΩ/m	T. Linnecar et al., 1993

date	Z_v in MΩ/m	Z_h in MΩ/m
13/08/1999	25 ± 6	-3.3 ± 0.7
23/08/1999	24 ± 2	-4.8 ± 0.7
17/09/1999	33 ± 3	-2.0 ± 0.4
10/11/1999	30 ± 2	-2.4 ± 0.3
weighted average	28 ± 2	-2.6 ± 0.2

Monitoring the SPS Impedance Upgrade

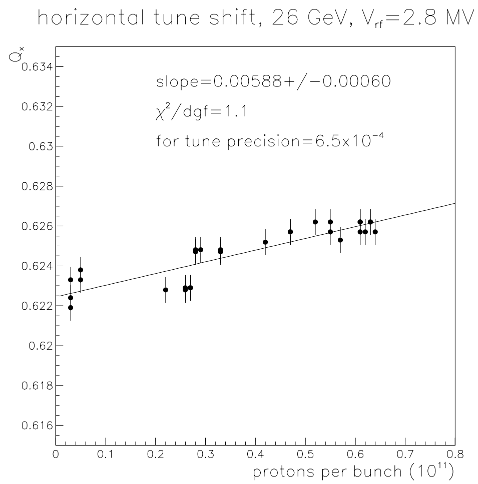

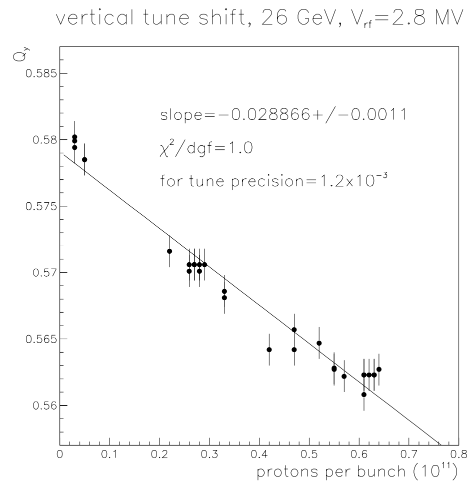

Measurement of $Q_{x,y}$ vs. N_b for single proton bunch at 26 GeV.
Broadband impedance model with $[R_s] = \Omega\ \mathrm{m}^{-2}$:

$$Z_1^{\perp} = \frac{c}{\omega} \frac{R_s}{1 + iQ\left(\frac{\omega_r}{\omega} - \frac{\omega}{\omega_r}\right)} \approx -i\frac{cR_s}{Q\omega_r},$$

$$\Delta Q \approx \frac{\beta_{x,y}}{4\pi}\left(\frac{-ieI\ \mathrm{Im}Z_1^{\perp}}{E}\right)$$

So, $\Delta Q/\Delta I \propto \Delta Q/\Delta N_b \rightarrow \mathrm{Im}Z_1^{\perp}$. Head-tail growth rates $\rightarrow \mathrm{Re}Z_1^{\perp}$.

LHC as Heavy Ion Collider

accelerator	RHIC	LHC
species	gold	lead
energy/charge E/Z [TeV]	0.25	7
energy/nucleon E/A [TeV]	0.1	2.76
total c.m. E_{CM} [TeV]	39	1148
dip. field B [T]	3.46	8.4
circumf. C [km]	3.83	26.66
#bunches n_b	57	608
ions per bunch N_b [10^7]	100	6.8
rms beam size $\sigma^*_{x,y}$ [μm]	110	15
beta function $\beta^*_{x,y}$ [m]	2	0.5
tune shift/IP $\xi_{x,y}$	0.0023	0.00015

acc.	RHIC	LHC
bunch length σ_z [cm]	18	7.5
spacing $L_{\rm sep}$ [m]	63.9	124.8
tr. emit. $\gamma\epsilon_{x,y}$ [μm]	1.7	1.5
long. emit.ϵ_L/Z [eVs]	0.12	0.2
IBS gr.t. $\tau_{\rm IBS}$ [hr]	0.4	9.8
init. lum. L [10^{27} cm^{-2}s^{-1}]	0.2	1.0
lum. lifet. τ [hr]	~10	9.3

Limitations for Heavy Ion Operation

- electromagnetic processes: e^+e^- pair production and subsequent e^- capture

  cross section $\sigma_c \approx 100$ barn for Pb^{81+}-Pb^{81+}, or $\dot{N}_c \approx 10^5$ ions s^{-1} per side of IP at $L \approx 10^{27}$ cm^{-2}s^{-1} $\sigma_c \propto Z^7$; energy deposition $\propto Z$

  ions which change charge state by 1 ($\Delta\delta = 1.2\%$ for Pb) are lost over about 1 m in the dispersion suppressor

  loss rate close to quench limit

  remedy: dynamic β squeeze? local collimators?

- for light ions longitudinal intrabeam scattering (IBS) growth time of 10 hours $1/\tau_{\rm IBS} \propto Z^3/A$

Initial luminosities: 1.0×10^{27} cm^{-2}s^{-1} Pb^{82}_{208}, 6.6×10^{28} cm^{-2}s^{-1} Kr^{36}_{84}, 3.1×10^{31} cm^{-2}s^{-1} O^{8}_{16}.

Intermediate Conclusions

- hadron colliders have performed exceedingly well in the past
- LHC will reach the highest energy (14 TeV) and highest luminosity (10^{35} cm^{-2}s^{-1}) ever
- LHC design is based on the experience gained at the ISR, SPS, Tevatron, HERA, RHIC,...; conservative assumptions

- yet accelerator physicists face exciting challenges, *e.g.*,
  - magnet technology and cryogenics
  - long-range collisions
  - strong-strong collisions
  - radiation damping stronger than IBS (tomorrow)
  - electron cloud (tomorrow)
  - demanding upgrade options (tomorrow)